Title
Exosomes regulate microglia activation during inflammation and aging

Author
Udeochu, Joe C.

Publication Date
2017

Peer reviewed|Thesis/dissertation

Exosomes regulate microglia activation during inflammation and aging

by

Joe C Udeochu

DISSERTATION

Submitted in partial satisfaction of the requirements for the degree of

DOCTOR OF PHILOSOPHY

in

Biomedical Sciences

in the

GRADUATE DIVISION

of the

UNIVERSITY OF CALIFORNIA, SAN FRANCISCO

DEDICATION AND ACKNOWLEDGEMENTS

Parts of chapter one are modified from material in Udeochu JC, Shea JM & Villeda SA. *Clin. And Exp. Neuroimmunol. 7(2): 114-125*. The research described in this dissertation is the result of hard work and support from a great team of scientists. I would first like to thank my mentor, Saul Villeda. Saul created a lab environment that allowed me to develop my technical and intellectual expertise, to establish an identity as a scientist and to contribute to the science community through conference presentations. These achievements would not be possible without a great lab team who have contributed to this project through many meaningful discussions. I would like to thank Jill Bouchard for taking me under her wing when I first joined the lab and bringing me up to speed on microglia techniques that were pivotal to the execution of my project. I want to specially acknowledge the two interns that came to work with me on this project, Alvan Cai and Cesar Sanchez-Diaz. Working with Alvan and Cesar was a great opportunity to give back what I have learned through hands-on mentorship and indeed made my graduate training a more fulfilling experience.

I would also like to thank other members of the science community that have guided me throughout my graduate training. From my first two rotations, Maureen Balestra, Anna Gillespie, and Sakura Minami, for helping me broaden my technical expertise at the bench and for helping ease my transition into grad school. I would also like to thank Michael McManus, Josh Robinson, and TJ Hu for very instrumental assistance during the developmental phase of this project. I owe a lot to Patricia Phelps, my undergraduate mentor, who gave me my first opportunity to learn about scientific research. Her foresight and attentive mentoring style has greatly shaped my approach to

work and passion for mentoring younger students. She continues to be a strong advocate for my career development, and I will be forever grateful. I would like to give a big shout out to the staff, mentors, fellows and students of the Neuroscience Scholars Program. The opportunity to be an NSP fellow has been a revolutionary experience for me. I have been fortunate to interact with a lot of great minds that share my passion about education, science and society. To my mentors at El Camino College – Teresa Palos, Elaine Moore, Brian Mims and the rest of the Umoja community – thank you for always keeping me grounded and connected to my roots.

I would like to thank members of the BMS program for creating a warm and friendly learning environment. The importance of having colleagues to talk to and relax with when a break from science is needed cannot to understated. I would also like to thank members of the larger UCSF community, particularly those affiliated with the Multicultural Resource Center, for providing avenues to meet other underrepresented students and for furthering discussions on making UCSF a more inclusive community.

Finally, I want to thank my family without whom I never could have done this. I want to thank my mom and dad for their continued investment in my development - I wouldn't be here without them. To my brother, Okey, with whom I emigrated with to the States in 2004, I am glad to have such a strong yet calming presence on my side for this entire ride. To Diane, Mimi, and Junior, thank you for your love and support which has not faded despite the distance between us. To my family in Carson, thank you for providing me a second home and much needed love in times of distress. To the youngest members of the family – Kamsi, David, Aliji, Jerry, Joe and Jacob – the sky is your horizon and I will also be there to support your dreams. Thank you!

Exosomes regulate microglia activation in acute and chronic age-associated inflammation

Joe C Udeochu

Microglia are important sentinels of brain homeostasis, involved in constant surveillance of brain tissue for debris, removal of apoptotic cells, and developmental sculpting of neuronal synapses. Drastic changes in brain homeostasis due to injury, disease or aging result in dramatic microglia responses, characterized by adoption of an activated phenotype resulting in increased production of inflammatory mediators. Effective communication is necessary not only for rapid responses to such perturbations but also to regulate the extent of response to minimize collateral tissue damage. Here, we comprehensively investigate a novel form of non-conventional vesicle communication involving exosomes and its roles in microglia inflammatory responses. We utilized a combination of proteomics, RNA sequencing, molecular targeting, pharmacology, genetic animal models and functional assays to explore the interactions between exosomes and inflammation in microglia. We found a unique bidirectional interaction between exosomes and inflammation. Microglia proinflammatory activation results in downregulation of exosome regulatory genes, *nSMase2* and *rab27a*, while anti-inflammatory activation promotes the expression of these genes. Consequently, we observe an increased representation of immune related proteins and microRNAs (miRNAs) in exosomes secreted by acutely activated microglia. These exosomes are able to act as direct mediators of inflammatory signaling between microglia, as cells treated with exosomes undergo dramatic gene expression and functional changes associated with activation such as upregulation of immune genes and enhanced phagocytic response. In addition,

microglia with impaired exosome release show a more activated phenotype characterized by prolonged expression of immune signaling genes. Mechanistically, this aberrant phenotype results partly from inadequate release of miRNAs, such as miR-155, during the resolution of inflammation in microglia with impaired exosome release. Finally, we identified increased exosome production as a hallmark of brain and microglia aging. Augmented exosome release in aged microglia serves to dampen the effects of aging-associated brain inflammation, as pharmacological blockage of exosome production results in a more exaggerated activation phenotype. Together, these findings highlight novel roles for exosomes in microglia immune responses and provides additional mechanistic insights into effector mechanisms utilized by microglia to resolve acute and chronic inflammation.

TABLE OF CONTENTS

Chapter 4: Materials and methods

LIST OF FIGURES

LIST OF TABLES

CHAPTER 1

INTRODUCTION

1.1 Microglia

Microglia are the resident immune cells of the brain, derived from erythromyeloid progenitors that populate the brain parenchyma at embryonic day 9 [1-3]. Following invasion of the brain parenchyma, these progenitor cells undergo a series of developmental changes, driven by epigenetic modifications that encode specific transcriptional and molecular signatures, to give rise to microglia [4,5]. Microglia phenotype is dictated both by their developmental origin as immune cells, as well as the tissue environment of the nervous system[6]. Consequently, microglia transcriptome and proteome consists of classical immune molecules such as cytokines, complement factors, and purinergic receptors[7,8], as well receptors and factors dedicated to nervous system support such as brain derived neurotrophic factor[9].

Due to technical limitations in the field of glia biology, there was a persistent lack of appreciation for the functional relevance of microglia in the brain. Recent advances in mouse genetics, live microscopy, and high throughput sequencing, however, have greatly revolutionized our understanding of microglia function in the brain[7,10,11]. Using newly developed technology of live brain imaging, Nimmerjahn and others provided the first ever visualization of microglia in live animal, using the fractalkine reporter mouse[11]. This study showed green fluorescent protein positive microglia to be very active in the brain, constantly exploring their microenvironment, making contact with neighboring cells, and phagocytosing extracellular debris. This observation stood in stark contrast to the long-held notion that microglia in the non-diseased brain were static and adopted a resting phenotype, and instead portrayed microglia as actively surveying cells in the brain. In addition to steady state surveillance, microglia are able to respond to perturbation of the

brain microenvironment by rapidly extending their processes to sites of injury and increased extracellular ATP[12]. Thus, these findings place microglia as central players in the maintenance of brain homeostasis, through continuous and active tissue surveillance.

Additionally, advances in mouse genetics have allowed scientists to directly investigate molecular mechanism involved in microglia interaction with and regulation of other brain cells. Microglia-specific gene deletions have identified important roles for microglia in regulating neuronal circuitry, developmentally as well as in the adult brain. Microglia expression of complement cascade proteins, such as the complement receptor 3 (CR3), is critical for proper development of neuronal circuitry in the visual cortex and other brain areas through a mechanism involving selected tagging and elimination of weak synapses to allow the persistence of stronger synapses[13]. Microglia have also been implicated in synapse formation. Deletion of microglia derived BDNF impairs motor neuron synapse formation, resulting in impairment in locomotive learning[9]. In addition, direct microglia contact on synapses can regulate synaptic activity. Microglia processes have been shown to reduce calcium signaling activity, a proxy for neuronal activity, in the zebrafish larvae following contact of processes with synapses[14]. These findings identify the diversity of microglia function in the brain and highlight the importance of microglia communication, via direct contact and secretion of factors, in regulating neuronal connection and activity.

1.2 Aging-associated microglia inflammation and dysfunction

Aging is the leading causal factor of many neurodegenerative disorders, such as Alzheimer's disease (AD), and is associated with increased incidence of impaired

information processing and recall. These aging associated functional changes occur in part due to impaired homeostasis resulting from dramatic changes in brain microenvironment and its cellular constituents, including microglia [15,16]. Microglia are particularly sensitive to homeostatic perturbation during age and neurodegenerative disease, as evident by dramatic changes in morphology, activation, and secretion (Figure 1). Accumulating evidence suggests that such changes interfere with microglia supportive functions, leading to synaptic dysfunction and consequently cognitive decline. Aberrant communication, characterized by increased production of immune molecules, has emerged as one mechanism driving microglia transformation in aging.

Global increases in the levels of pro-inflammatory cytokines, such as interleukin-1β (IL-1β), tumor necrosis factor α (TNFα) and IL6, are observed in the aged brain, indicating a heightened inflammatory status compared to the young brain. Given that microglia expression and production of inflammatory cytokines is much higher than other neuroglia, microglia are likely a major culprit driving age-related brain inflammation. Indeed, aged microglia produce higher levels of proinflammatory IL-1β, TNFα and IL6, indicative of a transformation from a surveying to an activated phenotype [17,18]. This phenotypic alteration is in part driven by epigenetic changes in aged microglia. For example, decreased levels of the epigenetic repressor, SIRT1, during aging partially mediates the increased transcription of *Il1β* in microglia and promotes senescence, both hallmarks of aging microglia[19]. In addition to affecting cytokine production, aging also alters the complement system in aged microglia. In both mice and humans, transcripts for various complement factors including *C1q*, *C3*, *C4*, *C3aR1*, and *C5aR1* are elevated in forebrains and hippocampi during normal aging and AD conditions [20-23]. Indeed, there

is evidence that aberrant complement activation can trigger excess synaptic pruning by microglia in aging[24] and preclinical stages of AD[25].

In addition to these changes in pro-inflammatory cytokine and complement production, aging microglia also display changes in morphology and process dynamics characteristic of classical pro-inflammatory activation. Aged microglia transform from ramified to amoeboid morphology, characterized by larger cell bodies and shorter dendritic processes, compared to young microglia that exhibit elaborate ramified processes and smaller cell bodies[15]. These changes are observed in various regions of the brain including the retina, hippocampus, forebrain, as well as visual and auditory cortices, suggesting a global response of microglia to aging. There is increasing evidence that these structural changes result in altered surveillance in aged microglia. Results of *in vivo* and *ex vivo* imaging studies have identified differences in process dynamics and motility between young and aged microglia [26,27]. For example, baseline process motility speed is reduced and ATP-induced changes in process motility and dendritic area are blunted in aged compared to young microglia [26,27]. Besides, aged microglia processes appear to respond differentially to stimuli - aged microglia respond to ATP by process retraction while young microglia respond by process extension[26].

Taken together, these observations highlight dramatic changes in microglia functional capacities in the aging brain and implicate enhanced inflammatory signaling as a major driver of these functional changes. Given the impact of enhanced inflammatory signaling on microglia homeostatic functions including surveillance, debris clearance, and production of trophic factors, there is a glaring need for better understanding of the molecular mechanisms underlying these functional changes and their impact on other

cells in the brain. Here, we focus on communication as regulatory axis for controlling microglia inflammation, restoring homeostatic functions and limiting collateral tissue damage due to persistent chronic inflammation during aging.

1.3 Exosomes

Extracellular vesicles (EVs) are membrane bound vesicles that have emerged as mediators of intercellular communication in numerous cell types including neurons, astrocytes, oligodendrocytes, neural stem cells, and microglia[28-31]. EVs exhibit heterogeneity in size and organelle of origin - microvesicles and apoptotic bodies range in size from 30nm to 1μm and are derived either from direct budding at the plasma membrane while exosomes form via endocytic maturation of the multivesicular body and are typically 30-150nm[28]. EVs contain a mixture of bioactive lipids, proteins and RNA molecules that can be transferred between cells to alter various biological responses under physiological and pathological conditions. Thus, EVs represent a novel mechanism of cell communication with potentially wide ranging influence on biology.

Indeed, exosomes have recently received a tremendous amount of attention in a range of diseases of the nervous system including glioma, Parkinson's disease, AD, and prion disease [32-35]. Most of these studies have focused on exosomes as potential biomarkers for disease given the presence of pathological markers such as amyloid beta (Aβ), tau, α-synuclein, superoxide dismutase, etc. in exosomes derived from brains, cerebrospinal fluid and blood of diseased patients and animal models of disease [36,37]. Exosomes have also been implicated in disease pathogenesis particularly in AD, with manipulation of exosome production resulting in altered amyloid plaque deposition and

tau propagation in animal models[38,39]. More recently, exosomes have also been studied for their role in regulation of neural and glia cells function in the absence of disease[40]. Transfer of exosome microRNAs partially mediates the effects of hypothalamic stem cells on systemic aging[40]. These studies show broad interactions of exosomes with brain disease and suggest exosome involvement in regulation of neuroglia physiology.

Microglia are an attractive cellular candidate to begin the investigation of exosome regulation of cellular function. First, due to their highly surveying and phagocytic nature, microglia are likely to interact with exosomes in the brain extracellular space. Indeed, microglia have been demonstrated to efficiently internalize exosomes produced by other neuroglia including neurons, astrocytes and oligodendrocytes *in vitro*[29,30]. Secondly, seminal work in the field of exosome biology has identified exosomes as potent regulators of various aspects of peripheral immune cell inflammatory responses including antigen presentation, phagocytosis, activation, and migration[41,42]. Owing to their role as primary immune cells of the brain, one stands to reason that some, maybe all, of these functions are regulated by exosomes in microglia. Proteomic analysis of microglia-derived microvesicles and exosomes provides some rationale for the involvement in microglia inflammatory responses. Microglia exosomes and microvesicles contain immune-modulatory molecules such as IL-1β proprotein and its processing enzyme, major histocompatibility proteins, cathepsins and integrins [43,44]. Whether or not microglia-derived exosomes can transfer such cargo to influence functional responses in the other cells remains to be assessed, and offers yet another potential mechanism of microglia inflammatory signaling.

1.4 MicroRNAs and exosomes

The novelty of exosome signaling is owed in part to the ability of these vesicles to transfer small RNAs that can regulate cellular responses. Of these small RNA species, microRNAs (miRNAs) are particularly enriched in exosomes[45]. miRNAs are a class of small non-coding RNAs that are produced from mRNA transcripts following sequential processing by endonucleases[46]. Pri-miRNAs produced following transcription are cleaved by DGCR8 and Drosha to produce pre-miRNAs that are further processed by the ribonuclease type III Dicer in the cytoplasm to produce mature miRNAs. Single stranded mature miRNAs associate with other proteins to form RNA induced silencing complexes (RISC), which bind to target mRNAs based on sequence complementarity resulting in mRNA cleavage or translation inhibition[47]. miRNA mediated post-transcriptional regulation of gene expression has been implicated in many aspects of biology including development[48], cellular identity and cellular responses[47].

The observation of miRNA enrichment in exosomes has raised questions about its functional relevance – does the enrichment serve as a mechanism for signaling by extracellular RNAs or does it demonstrate additional cellular mechanisms involved in miRNA biogenesis and target recognition? Exosomes can transfer biologically active miRNA species between cells[49] resulting in target gene repression and altered responses involved in suppression of inflammation[50] and tumor metastasis[35] *in vivo*. Additionally, exosomes have been implicated in the assembly and disassembly of miRNA-RISC complexes thus affecting miRNA target recognition in a cell autonomous manner[51]. These observed functions of exosomes in miRNA regulation of gene transcription are yet to be

studied in the context of microglia inflammation, and could serve as additional arsenal in microglia immune response repertoire.

1.5 Aims of this study

Microglia have long been appreciated as the primary immune cells of the brain that respond to a diverse array of perturbations, systemically and locally in the brain. Though rapid microglia response to perturbation often serves a protective function, prolonged inflammatory activation can have detrimental effects on other brain cells and resulting in impaired function. Despite advances in the field, there still remains a paucity of knowledge of intrinsic regulatory mechanisms utilized by microglia to control the degree of inflammatory activation. The goal of this study was to understand the roles of exosomes and miRNAs in regulating acute and chronic aging-associated inflammation in microglia. We utilized RNA sequencing, mass spectrometry and transcriptional profiling of exosomes and microglia to understand the composition of exosomes and dynamics of exosome cargo in microglia during inflammation. These approaches informed the development of *in vitro* and *in vivo* molecular, pharmacological and genetic approaches utilized to provide comprehensive insights linking exosomes and miRNAs in regulating gene expression and magnitude of microglia inflammatory responses.

Figure 1

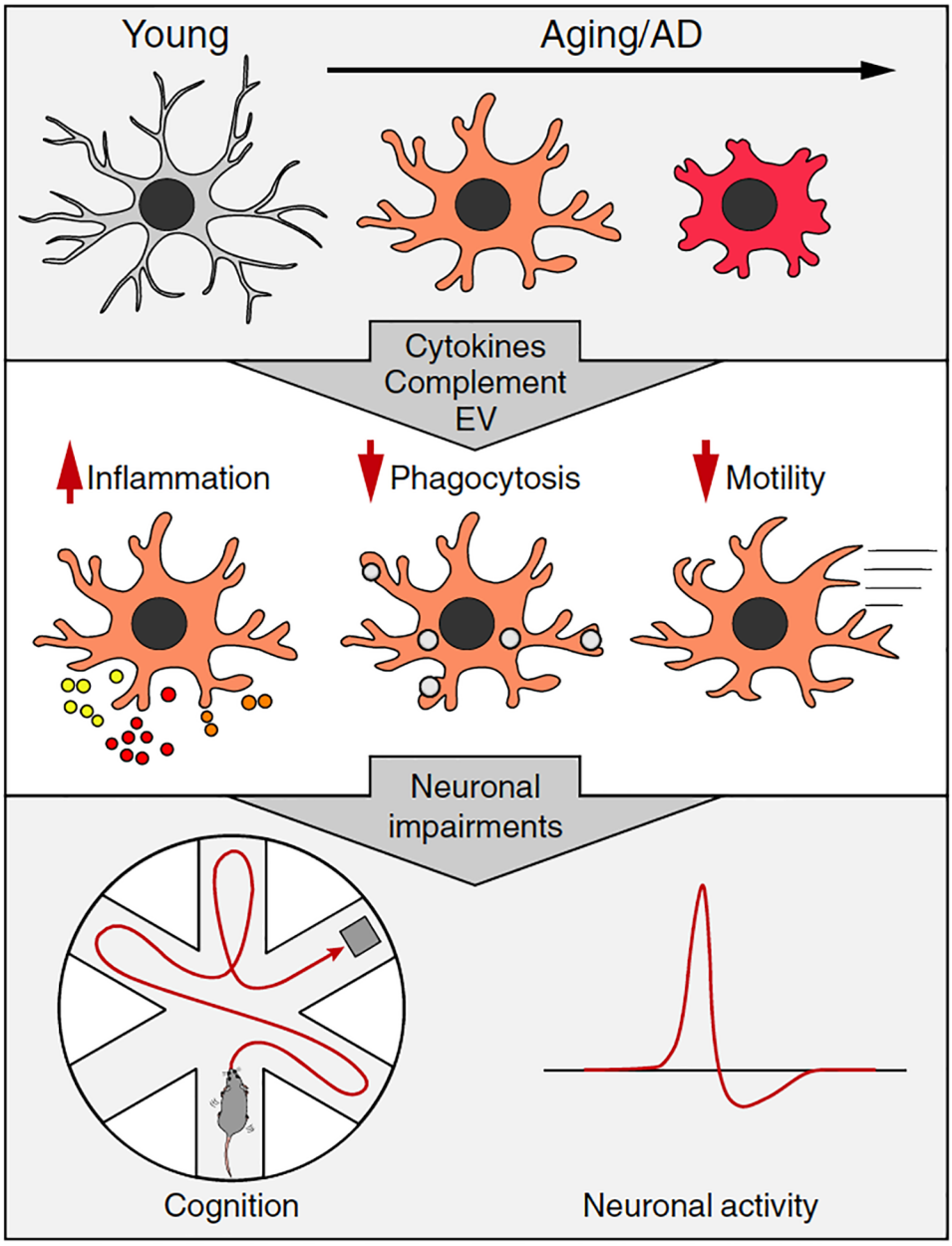

Figure 1: Schematic demonstrating the interaction between microglia aging and impaired cognition in aged animals. Activation induced changes in microglia morphology and functions drive impaired synaptic function contributing to behavioral impairments.

CHAPTER 2:

EXOSOMES REGULATE MICROGLIA ACTIVATION DURING INFLAMMATION AND AGING

2.1 Abstract

Proper regulation of inflammatory responses is critical for effective microglia function in physiology and disease. While much emphasis is placed on mechanisms driving microglia activation, there remains a gap in knowledge on how microglia resolve or modulate inflammatory activation. Here we provide a comprehensive analysis of exosome regulation of microglia inflammatory response, highlighting a novel anti-inflammatory function of exosomes. First, microglia-derived exosomes contain immune molecules that are sufficient to propagate signals driving transcriptional changes associated with increased inflammatory cytokine production and phagocytic clearance in recipient microglia. Secondly, microglia with impaired exosome biogenesis display altered inflammatory kinetics, characterized by exaggerated and prolonged expression of pro-inflammatory molecules in response to acute and chronic aging-associated inflammation. This robust anti-inflammatory function of exosomes is manifested in part through the release of proinflammatory microRNAs, such miR-155. Taken together, our study identifies exosomes as critical mediators of inflammatory communication in the brain that play important roles in intracellular resolution of microglia inflammation.

2.2 Significance

Inflammation is a hallmark of brain aging and various neurodegenerative conditions, and contributes to functional impairments associated with these conditions. Understanding the nature of inflammation induced changes, globally and cell autonomously, will greatly inform therapeutic strategies aimed at preserving and/or restoring impaired functions in aged and diseased brains. Here, we show that microglia exhibit remarkable plasticity in

their response to inflammation, upregulating genes and cellular processes such as exosome production, necessary to counterbalance the effects of acute and chronic activation. This study identifies the induction of enhanced exosome release as a novel as an anti-inflammatory mechanism involved in the restoration of microglia homeostasis following activation, thus establishing a network linking gene expression, miRNAs, exosomes, and inflammation.

2.3 Introduction

Microglia activity and function are strongly tailored to meet their specialized functions as the tissue macrophages of the brain [11,52]. Like other tissue macrophages, microglia are able to respond to changes in their environment, produce recruitment and activation factors, and engage phagocytic mechanisms in order to restore homeostasis [53,54]. While great advances have been made in understanding microglia developmental origin [1-3], regional heterogeneity [55], pathological and non-pathological transcriptional networks [8,56], much still remains to be learned about the mechanisms that allow microglia to manifest such degree of cellular and functional plasticity in the brain while maintaining a relatively low immune activation profile. Proper inflammatory regulation following microglia activation is necessary for effective microglia responses, minimizing brain tissue damage and alterations to neural networks associated higher order functions. These mechanisms of homeostatic resolution are even more pressing under conditions that drive chronic microglia activation such as disease, infection and aging.

To broaden our understanding of mechanisms of immune resolution in microglia, we focus here on the involvement of vesicle transport, specifically involving exosomes, in

the regulation of microglia inflammatory responses. Exosomes are a subset of endosomal-derived extracellular vesicles (EVs), that are produced by invagination of the limiting membrane of the multivesicular body (MVB) and released into the extracellular space upon fusion of the MVB with the plasma membrane [28,42]. Exosomes have been implicated in various cellular processes including removal of debris and transfer of bioactive proteins, lipids, and RNA molecules. The latter has emerged as an important regulatory mechanism in various stages of peripheral immune response including inflammatory activation and suppression, antigen presentation, and phagocytosis [41,49,50,57,58]. Given these associations with peripheral immune responses, expression of immune molecules in microglia-derived exosomes [43], and the proficiency of exosome uptake by microglia [29,30], we decided to explore the roles of exosomes in microglia inflammation. We hypothesized that exosome production is critical for proper microglia inflammatory responses, and investigated mechanisms involved in exosome signaling and their roles in age-associated chronic microglia activation.

Our studies show that microglia exosome production is regulated by inflammation, based on activation induced changes to both exosome content and the expression of exosome regulatory genes. Functionally, we demonstrate two important immune regulatory roles for exosomes in activated microglia. First, exosomes can directly transfer molecules that result in immune activation of recipient microglia, resulting in transcriptional and functional changes. Secondly, induction of exosome release is critical for efficient resolution of inflammation in microglia via the regulation of the intracellular abundance of immune miRNAs such as miR-155. Inhibition of exosome production during

acute and chronic age-associated inflammation exaggerates microglia activation, highlighting a novel and robust anti-inflammatory mechanism in microglia.

2.4 Results

2.4.i Microglia exosome production is regulated by the ceramide synthase pathway and rab GTPases, via nSMase2 and rab27a

Given the novelty of the field of exosome biology at the inception of this project, we relied heavily on *in vitro* platforms to gain insights into exosome function in microglia. Consequently, we utilized cultured microglia-like cell line, BV2, and primary microglia derived from postnatal mouse brains for purification of extracellular exosomes and for subsequent downstream functional analyses.

To begin our study, we first confirmed microglia production of exosomes by primary and BV2 microglia grown overnight in serum-free media. Exosomes were isolated from growth media by standard filtration and differential ultracentrifugation protocol as previously described [59], and analyzed. Analyses of the isolated vesicles revealed physical characteristics typical of exosomes. Microglia exosomes exhibited classic donut-shaped morphology as determined by scanning electron microscopy and were mostly in 30-150nm size range based on nanoparticle tracking analysis (NTA) (Figure 2.1A, B). Previous studies[60] have identified expression of tetraspanin proteins and endocytic process as protein markers that distinguish exosomes from other types of extracellular vesicles. Western blot of microglia exosomes confirmed the expression of tetraspanin proteins, CD9 and CD63, and expressed endolysosome associated, LAMP2 protein

(Figure 2.1C). Thus, we confirmed the isolation of exosomes from our microglia cultures based on physical properties and protein expression.

To determine molecular mediators of microglia exosome production, we targeted the ceramide synthase pathway and rab27a GTPase in microglia exosome production. Pharmacological targeting of the neutral sphingomyelinase 2, nSMase2, using the sphingomyelinase inhibitor, GW4869, resulted in reduced exosome production in treated compared to control microglia as determined by NTA (Figure 2.1D). Additionally, we developed a lentiviral mediated short hairpin RNA (shRNA) strategy for targeting rab27a (Figure 2.1E). BV2 microglia were transduced with lentiviral particles expressing scramble (scm) or rab27a targeting (kd) short hairpins and treated with puromycin for positive selection (Figure 2.1F). Subsequent analysis of rab27a transcript levels by quantitative PCR (qPCR) confirmed efficient knockdown of *rab27a* expression (Figure 2.1G) Analyses of exosome production in scm and kd BV2 revealed significantly less exosome production in kd compared to scm BV2 microglia (Figure 2.1H-J). Thus, exosome production and release in microglia is an active process involving nSMase2 and rab27a GTPase function.

2.4.ii Expression of exosome regulatory genes is partially regulated by microglia activation state

To gain insights into the involvement of exosomes in microglia responses to inflammation, we probed the expression profiles of nSMase2 and rab27a in microglia stimulated with inflammatory agents - interferon gamma (IFNγ), lipopolysaccharide (LPS), or polyribocytidilic acid (poly I:C). Microglia were collected and analyzed by quantitative PCR at 6 and 24 hours following stimulation in order to monitor the kinetics of gene

expression (Figure 2.2A-C). As expected, IFNγ, LPS and poly I:C triggered strong changes in microglia expression of inflammatory cytokine genes, *IL1β, TNFα,* and *IL4*. Remarkably, the expression of exosome regulatory genes, *nSMase2* and *rab27a,* were also altered by microglia activation, with each stimulating agent producing slightly different patterns of change. Of particular interest is the observation that *rab27a* expression pattern followed similar kinetics as the anti-inflammatory gene, *IL4* under all stimulating conditions. This prompted us to ask if *rab27a* expression is regulated by IL4 signaling. Strikingly, acute IL4 stimulation resulted in upregulation of both *rab27a* and *nSMase2* compared to control and IFNγ-treated microglia (Figure 2.2D). These gene expression results show that exosome regulatory genes are responsive to microglia activation state and suggest possible antagonism between sustained exosome release and microglia activation.

2.4.iii Microglia activation results in increased recruitment of inflammatory proteins and microRNAs into exosomes

Given the physiological and pathological roles of interferon signaling [61-64], we focus on IFNγ regulation of exosomes in microglia from here on. To directly assess the roles of exosomes during microglia IFNγ inflammation, we first analyzed microglia exosomes for the presence of immune molecules. Exosomes isolated from BV2 microglia cultures following overnight incubation with or without IFNγ were pooled from several experiments and exosomal proteins and RNAs were isolated for analyses by mass spectrometry and megaplex qPCR profiling respectively. Label free liquid chromatography mass spectrometry revealed that BV2 microglia exosomes contained a heterogeneous mixture

of proteins including proteins typically enriched in exosomes, as determined by data mining in Vesiclepedia, such as Alix, lactachedrin, and ApoE, as well as proteins indicative of the myeloid and immune origin of the secreting cells mannose receptor, macrophage inhibitory factor, and integrin beta 2 (Table 2.1). Categorization of microglia exosome proteins confirmed heterogeneity of cargo, as various functional classes were represented including structural proteins, receptors and enzymes (Figure 2.3 A,B). Additionally, overrepresentation analysis revealed presence of proteins involved in processes such as cytoskeletal rearrangement, integrin signaling, and chemokine-cytokine signaling, suggesting a strong immune signature in microglia exosome proteins (Figure 2.3C). Although exosomes from unactivated and IFNγ activated BV2 shared many proteins, we observed activation-induced recruitment of immune-related molecules, some of which have been previously implicated in IFNγ responses such as CD28 and beta-2-microglobulin (Figure 2.3D).

Megaplex qPCR profiling revealed similar heterogeneity in microglia exosomal miRNA content (Table 2.2). miRNAs identified included those enriched in microglia relative to other neuroglia such as miR-146a, miR-342-3p, miR-125b-5p and miR-150 [65,66]. Additionally, there was also evidence of activation induced reorganization of microglia exosome miRNA cargo (Figure 2.3 E,F). IFNγ activation increased recruitment of miRNAs implicated in proinflammatory activation in microglia and other immune cells such as miR-155 and miR-142-5p (Figure 2.4 E,F). These results show that exosome cargo loading is an active process that can be modulated by the inflammatory state of microglia, resulting in increased abundance of immune modulatory proteins and miRNAs.

2.4.iv Exosomes from activated microglia are sufficient to propagate inflammatory signals to recipient cells result in gene expression changes

Given this observed recruitment of immune molecules to exosomes from activated microglia, we investigated two possible mechanisms of exosome modulation of microglia inflammation – the direct transfer of inflammatory cargo via exosomes to promote activation in neighboring cells and secondly, the release of exosome associated immune molecules as a mechanism of promoting restoration of homeostasis following microglia activation. We tested the first scenario by performing direct stimulation assays with purified IFNγ exosomes. Uptake of exosomes was confirmed by flow cytometry and confocal imaging of microglia treated overnight with exosomes labeled with the fluorescent dye (Figure 2.4 A,B). Uptake assays performed in the presence of catecholamine D or pitstop2 revealed that microglia exosome uptake occurs via actin- and clathrin dependent mechanisms (Figure2.4C).

Having confirmed uptake of exosomes by microglia in our stimulation paradigm, we next investigated the functional consequences of exosome uptake on recipient microglia. Stimulation assays were performed at 10:1, 20:1 and 30:1 ratios of secreting to recipient cells in order to establish a dose response range in recipient microglia. While stimulation with IFNγ exosomes at 10:1 ratio was well tolerated by recipient microglia, higher stimulation ratios resulted in inflammatory activation (Figure 2.5 A,B). Microglia treated with 30:1 of activated exosomes expressed higher transcript levels of *IL1β* and *TNFα* than vehicle-treated controls (Figure 2.5B). In addition, these cells displayed increased inflammatory signaling based on higher levels of NFκB p65 phosphorylation (Figure 2.5C,D). Recipient primary microglia were analyzed by high throughput RNA

sequencing to broadly characterize transcriptional signatures driving this observed exosome induced activation (Figure 2.6A). Ontology analysis of differentially expressed genes yielded terms such as response to interferon gamma and macrophage activation, indicating that exosomes effectively propagated of IFNγ signaling in recipient microglia (Figure 2.6B). Indeed, the top differentially expressed genes identified by RNA sequencing contained genes involved in IFNγ signaling (*Gbp2*) and IFNγ effector functions (*Ccl5* and *C3*) (Figure 2.6C,D). Taken together, our data show exosomes as novel mechanism of intercellular communication sufficient to promote enhanced immune activation in microglia by increasing transcription of inflammatory genes.

2.4.v Exosome production is necessary for efficient microglia phagocytosis in vitro

We next asked the functional consequences of exosome mediated inflammatory activation in microglia. Further inspection of differential enriched gene list revealed an enrichment of genes involved in phagocytosis. We identified genes involved in both complement and Fc gamma receptor mediated phagocytosis among genes that were upregulated by exosome stimulation, as well as cytoskeletal rearrangement as a significantly overrepresented pathway in exosome protein content. Consequently, we analyzed microglia morphological and phagocytic responses to exosome stimulation. Using *in vitro* live microscopy of exosome- and vehicle-treated microglia, we asked if exosome treatment resulted in any appreciable differences in microglia morphology (Figure 2.7A). We observed that exosomes promoted dramatic membrane rearrangement in recipient microglia resulting in a significant decrease in microglia with rounded morphology and an increase in microglia with ramified morphology (Figure 2.7B). To test

if these morphological changes were accompanied by increased microglia phagocytosis, we performed *in vitro* latex bead assays. Primary microglia were treated with pre-opsonized latex beads and then analyzed (Figure 2.7C). We observed a dose dependent increase in microglia bead uptake in line with the transcriptional changes identified above (Figure 2.7D). To further validate these findings, we analyzed microglia phagocytosis in the two models of exosome depletion discussed in Figure 2.1. Rab27a knockdown and overnight inhibition of nSMase2 resulted in decreased latex bead uptake compared to respective controls. Thus, exosomes are critical for efficient microglia phagocytosis, suggesting a possible role for exosomes in microglia homeostatic clearance in the brain.

2.4.vi Exosomes are important for efficient resolution of microglia inflammation

To further validate the observed phenotype of exosome induced propagation of microglia inflammation, we asked the consequences of reducing exosome release during microglia IFNγ response. Rab27a knockdown (kd) and scramble (scm) BV2 microglia were treated with IFNγ and proinflammatory cytokine, JAK-STAT and toll like receptor signaling genes were analyzed 6 and 24 hours post stimulation, denoted here as activation and resolution phases respectively (Figure 2.8A). Impaired exosome release via rab27a knockdown minimally affected the initial response to IFNγ. Of the transcripts measured, only *TNFα* expression was significantly reduced in kd compared to scm microglia (Figure 2.8B). This observation suggests exosome release is necessary specifically for TNFα induction, not for global microglia activation downstream of IFNγ.

Remarkably, rab27a kd microglia exhibited more prominent alterations in expression of inflammatory genes during the resolution of IFNγ-induced activation. Kd

microglia maintained a more activated phenotype relative to scm microglia, evidenced by higher *IL1β*, *Stat1,* and *myd88* transcript levels in the resolution phase (Figure 2.8B). To confirm this observation, we repeated the IFNγ activation timecourse in GW4869 and vehicle treated BV2 microglia (Figure 2.8C). Although GW4869 had a less pronounced effect on IFNγ microglia inflammation, we observed significantly higher *Stat1* transcript levels during the resolution phase in GW4869 microglia compared to controls. These gene expression changes corresponded with altered Stat1 signaling in IFNγ treated rab27a kd and GW4869 microglia (Figure 2.8D,F). Stat1 phosphorylation was higher in IFNγ treated rab27a kd and GW4869 microglia compared their respective controls (Figure 2.8E,G). Taken together, we show that exosome release plays an indispensable role in resolution of inflammation in acutely activated microglia.

2.4.vii Exosomes promote inflammatory resolution in activated microglia partially through release of inflammatory microRNAs

Next, we sought to identify mechanisms underlying the aberrant resolution of inflammation in microglia impaired in exosome release. Given data above showing that immune molecules are recruited to exosomes of activated microglia (Figure 2.2), we hypothesized that reduced exosome-associated release of these molecules would result in increased intracellular retention contributing to aberrant inflammatory resolution. To test this hypothesis, we performed overnight IFNγ stimulation followed by qPCR analyses to measure cellular abundance of miRNAs that were either increased in abundance (miR-155) or specifically recruited to IFNγ exosomes (miR-103 and miR-142-5p). The cellular abundances of all three miRNAs were higher in IFNγ stimulated kd microglia compared

to scm microglia, with miR-155 being the most dramatically increased (Figure 2.9A). Additionally, miR-142-5p and miR-155 levels were also higher in IFNγ treated GW4869 microglia compared to control (Figure 2.9B). These observations suggest that inhibition of exosomes alters miRNA trafficking in activated microglia. To determine the consequences of this observed impairment in miRNA trafficking, we next asked if miRNA target expression is also altered in rab27a and GW4869-treated microglia. We focus on suppressor of cytokine signaling (SOCS1), an important negative regulator of interferon induced JAK/STAT signaling [67]. Interestingly, miR-155 acts as a positive regulator of interferon mediated microglia activation, partly by repressing SOCS1 expression [68,69]. qPCR analyses of *SOCS1* revealed significantly reduced expression levels in IFNγ-treated rab27a kd and GW4869 microglia compared to respective controls, confirming reduced expression of miR-155 targets in acutely activated microglia with impaired exosome releases (Figure 2.9 C,D). These observations highlight novel interactions between exosomes and miRNA transport, wherein exosome-mediated transport is critical for regulating intracellular abundance of inflammatory miRNAs in activated microglia. Thus, exosome-mediated miRNA transport represents a novel anti-inflammatory mechanism utilized by microglia to promote resolution of inflammatory activation.

2.4.viii Brain aging alters the abundance and size of interstitial exosomes

To broaden the physiological relevance of these observations, we next investigated the involvement of exosomes in regulating aging-associated microglia inflammation. Microglia aging is accompanied by increased production of inflammatory molecules resulting in a chronic state of activation that drives morphological and functional changes

in microglia [15,16,18]. Recent studies have shed some light on transcriptional changes underlying aging associated microglia activation, highlighting upregulation of interferon signaling and other antiviral responses as augmented in aged compared to young microglia [55,62]. In light of our findings implicating exosomes in regulation of interferon responses, we asked if and how exosomes are involved in regulating chronic microglia activation during aging. To begin, we compared young and aged brains for global changes in exosome production and release, using a previously published method for isolating brain interstitial exosomes [37]. Brain exosomes showed characteristic size and tetraspanin protein expression, based on nanoparticle and Western blot analyses (Figure 2.10 A,D). We observed size and protein expression differences in exosomes isolated from aged relative to young brains. Aged brain exosomes expressed higher levels of CD9 and CD63 compared to young brain exosomes (Figure 2.10 B,C). Nanoparticle analyses confirmed that this increase in protein expression was in part due to increased exosome numbers in aged compared to young brains (Figure 2.10 E). In addition, exosomes from aged brains displayed altered size distribution compared to young brain exosomes. Aged brain exosomes contained more vesicles in the 100nm size range, resulting in a significant reduction in mode vesicle size (Figure 2.10F). These findings show that brain aging is associated with changes to both the abundance and size of interstitial exosomes.

2.4.ix Aged microglia upregulate exosome production, partly as a consequence of impaired lysosomal function

To directly test the effects of aging on microglia exosome production, we utilized qPCR analysis of exosome regulatory genes in acutely isolated young and aged

microglia. This approach was taken in order to circumvent the challenge of isolating sufficient number of microglia to permit direct comparison of exosome numbers between the two aged groups. We first validated that isolated microglia displayed characteristic inflammatory changes. Indeed, aged microglia expressed higher transcript levels of *IL1β* and *IL10,* indicating a more activated state compared to young microglia (Figure 2.10A). Interestingly, *rab27a* expression was also significantly higher in aged compared to young microglia, suggesting that microglia activation in the aged brain is accompanied by enhanced exosome release (Figure 2.10A).

Furthermore, we analyzed intracellular structures involved in exosome biogenesis to determine if these changed with microglia aging as well by performing immunofluorescence labeling of teteraspanin (CD63) and endolysosomal proteins (CD68 and LAMP2) with microglia marker, Iba1, in young and aged brain sections (Figure 2.10B-D). Aged microglia expressed significantly higher levels of CD63, CD68 and LAMP2 relative to young (Figure 2.10E-G). These findings suggest that aging triggers changes in organelle structures involved in microglia exosome production. Given the role of the endolysosomal system in exosome biogenesis[42] and reported dysregulation of this system in aged microglia[24], we hypothesized that lysosome dysfunction partly drives augmented exosome production in aged microglia. As a proof of principle, we treated BV2 microglia cultures with leupeptin, an inhibitor of lysosome proteolytic activity and compared exosome production between treated and non-treated cells. Leupeptin treatment recapitulated phenotypes observed in aged microglia, such as altered CD63 expression pattern and increased *rab27a* levels, and also resulted in increased exosome release (Figure 2.10H-K). Taken together, our findings reveal increased exosome

production as a novel aspect of microglia aging, driven partially by impaired lysosomal function and increased inflammation.

2.4.x Enhanced exosome release in aged microglia serves an anti-inflammatory function of dampening microglia activation due chronic inflammation

Next, we asked if augmented exosome release plays any roles in modulating inflammation in aged microglia given our *in vitro* findings. To do this, we performed stereotaxic injections of GW4869 or vehicle into contralateral cortices or hippocampi in 3, 18 and 26 month mice (Figure 2.11A). Brains were harvested one week post injections and microglia activation analyzed by immunofluorescent labeling of CD68 (Figure 2.14B-E). We observed an age-dependent effect of blocking exosome production on microglia activation. In 3-month old injected brains, microglia expression of CD68 was similar on both GW4869- and vehicle- injected hemispheres (Figure 2.14F). In both 18- and 24-month old brains, however, CD68 expression was significantly higher in brain hemispheres injected with GW4869 compared to vehicle injected hemispheres CD68 (Figure 2.14G-H). These observed increases in microglia activation due to blockage of exosome production suggest that exosomes are necessary for dampening, not propagating, microglia inflammation in the aged brain. Thus, we can conclude that exosomes are a novel anti-inflammatory mechanism important for efficient microglia resolution and modulation of inflammatory activation in response to both acute and chronic age-associated inflammation.

2.5 Discussion

Microglia activation is indispensable to their role as central regulators of homeostasis in the brain. Here, we identify exosomes as novel cellular mediators of microglia homeostasis during inflammation. We show that exosome regulatory genes, *nSMase2* and *rab27a*, are sensitive to microglia activation. Functionally, augmented expression of exosome regulatory genes results in increased recruitment of immune molecules in exosomes. Inhibition of this process, either pharmacologically or using molecular approaches, results in retention of immune related molecules, such as miR-155. Consequently, activated microglia with impaired exosome production are defective in resolution of inflammation, showing prolonged expression of proinflammatory genes and activation of proinflammatory signaling pathways. This exosome mediated regulation of microglia activation is relevant for resolving acute inflammation, such as that induced by stimulation with proinflammatory IFNγ, as well as in modulating microglia activation under chronic aging-associated inflammation. Thus, exosome production is broad effector mechanism for promoting anti-inflammatory responses in activated microglia.

Figure 2i

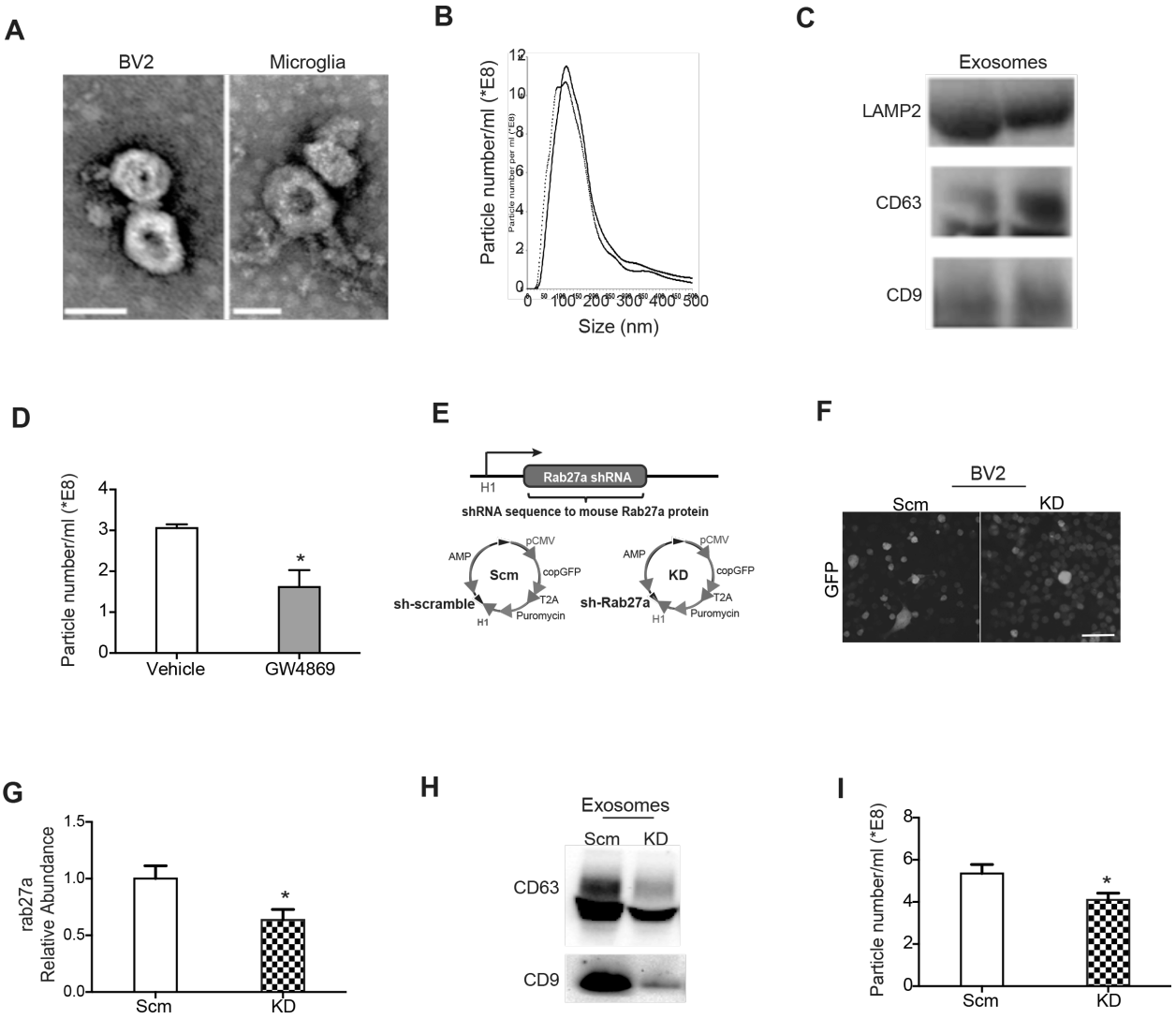

Figure 2.1. Microglia inflammatory activation regulates expression of exosome regulatory genes

(A) Representative electron micrographs showing prototypical cup-shaped morphology and size of BV2 and primary microglia exosomes (Scale bar = 50nm). (B) Nanoparticle tracking analysis of replicate exosome preps shows heterogeneous vesicle size, with most abundant vesicles ranging in size from 50 – 130nm. (C) Western blot analysis of

exosome lysates showing expression of tetraspanin (CD9 and CD63) and endocytic (LAMP2) proteins.

(D) Inhibition of neutral sphingomyelinase 2 (nSMase2) by GW4869 results in reduced microglia exosome production. (E) Schematic representations of rab27a (KD) or control (Scm) shRNA vectors with a green fluorescent protein (GFP) reporter. (AMP: ampicillin, pCMV: cytomegalovirus promoter). (F) Representative images of scm and kd BV2 microglia showing expression of green fluorescence protein reporter (G) qPCR validation of reduced rab27a expression in kd microglia relative to scm microglia. (H,I) Decreased rab27a expression results in decreased exosome production as determined by as determined by Western blot and nanoparticle tracking. All data represented as mean ± SEM; *P<0.05, t-test (D, G, I).

Figure 2ii

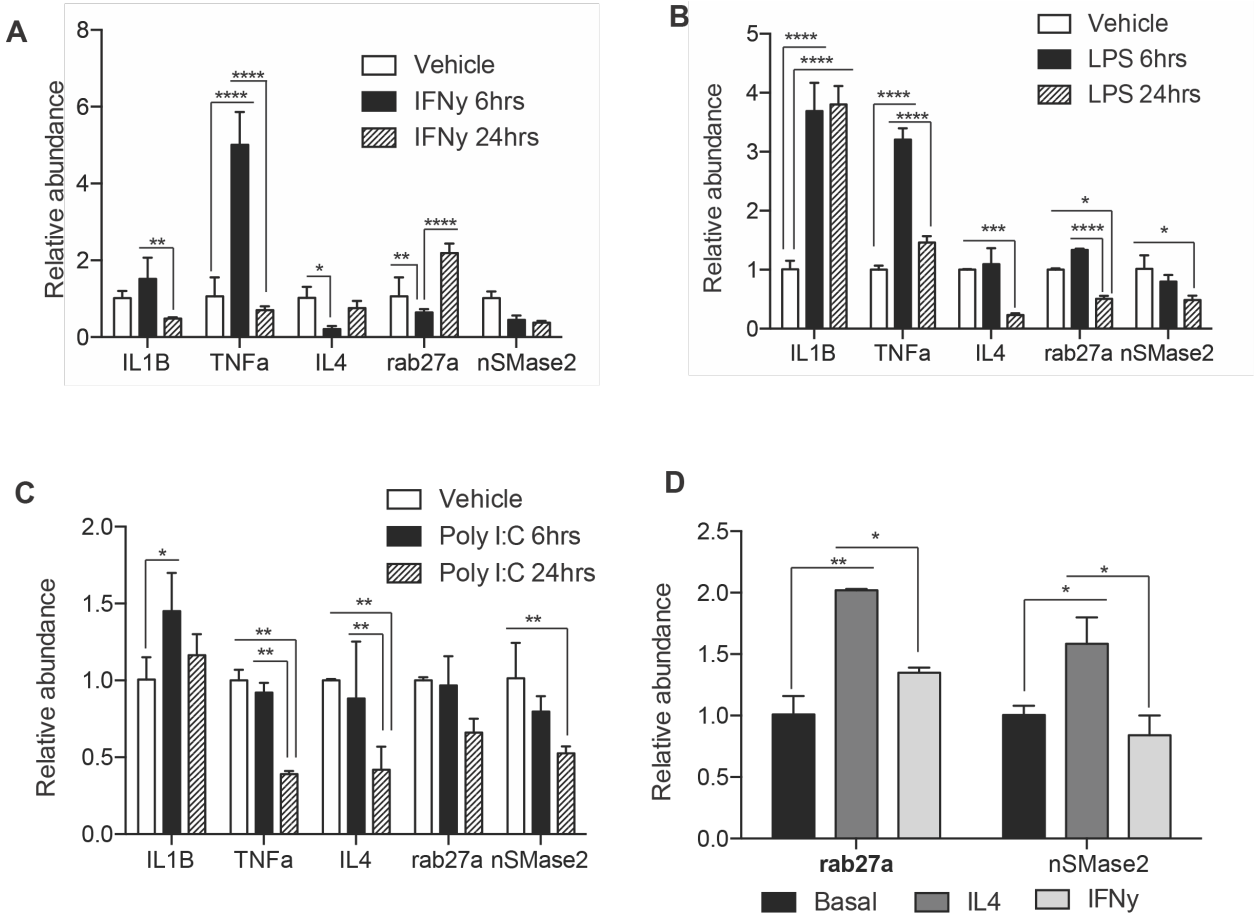

Figure 2.2: Characterization of activation induced changes in the expression of exosome regulatory genes

Microglia were treated with proinflammatory agents interferon gamma (IFNγ), lipopolysaccharide (LPS) or polyribocytidilic acid (poly I:C) to mimic microglia response to bacterial and viral agents. (A-C) qPCR was performed on RNA isolated from microglia at 6 and 24 hours post activation and compared to RNA isolated from unactivated microglia showing activation induced changes in inflammatory cytokine (*IL1β*, *TNFα, IL4)* and exosome regulatory (*nSMase2* and *rab27a*) gene expression. (D) qPCR analysis of microglia acutely activated by proinflammatory cytokine, IFNγ or anti-inflammatory

cytokine, IL4, showing IL4 induced upregulation exosome regulatory gene expression. All data represented as mean ± SEM; *P<0.05; **P<0.01; ****P<0.0001, t-test (A-D).

Figure 2iii

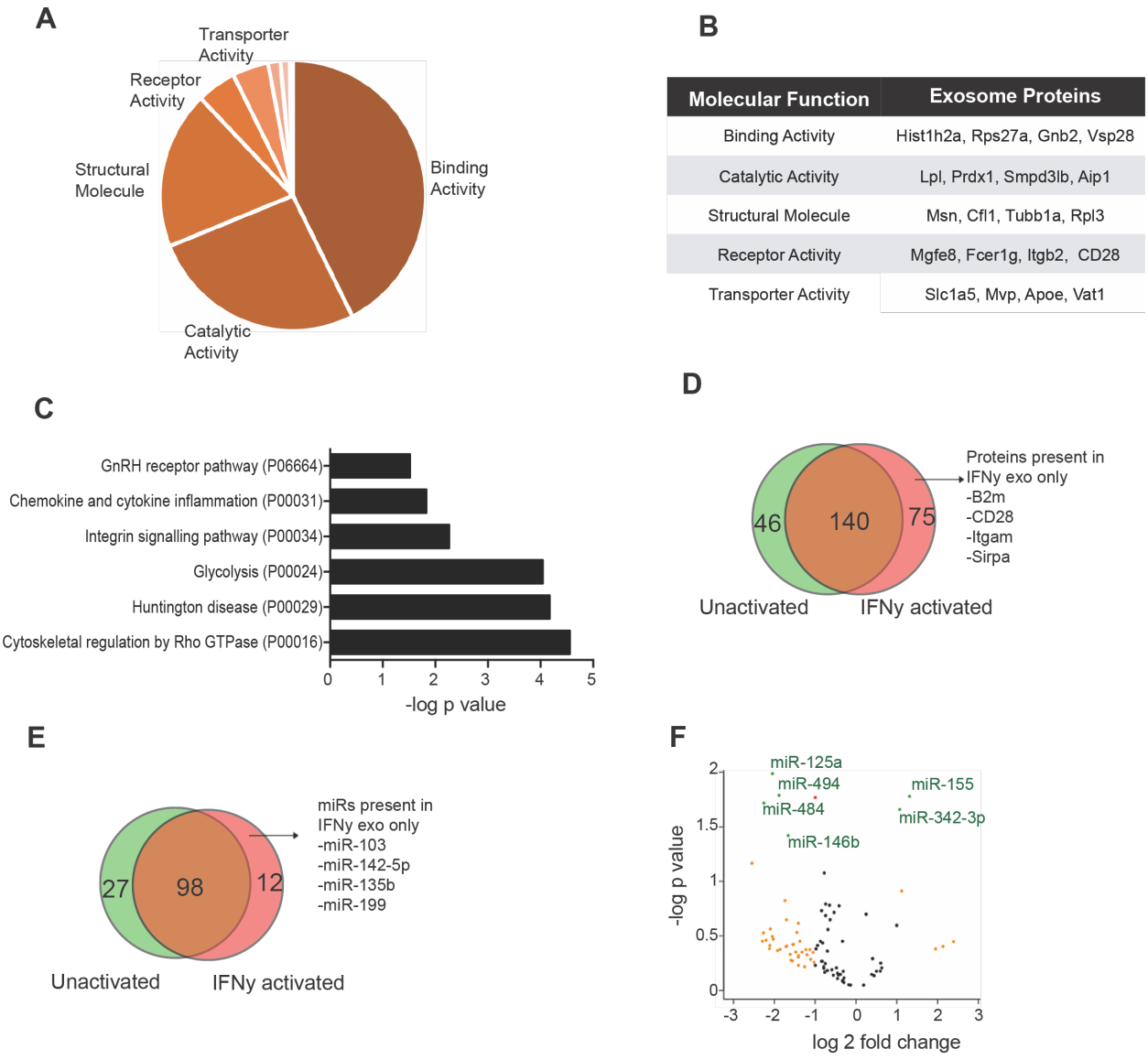

Figure 2.3: BV2 microglia exosome cargo is enriched in inflammatory proteins and microRNAs

(A) Pie chart showing heterogeneity in BV2 microglia exosome protein content. Proteins are displayed based on molecular function classification. (B) Corresponding examples of exosome proteins found in each functional classification. (C) Venn diagram showing number of proteins found in exosomes derived from unactivated and IFNγ activated

microglia. (D) Panther overrepresentation analyses of microglia exosome proteins showing significantly represented pathways, many of which are implicated in inflammatory response. (E) Venn diagram showing number of miRNAs found in exosomes derived from unactivated and IFNγ activated microglia. (F) Volcano plot showing IFNγ induced enrichment of immune related miRNAs, miR-155 and miR-342-3p, in IFNγ exosomes compared unactivated exomes (yellow = 2 fold change, red = $p < 0.05$, green = 2 fold change and $p < 0.05$). Bonferroni correction for multiple testing used to identify overrepresented proteins, $p<0.05$ (D,F), t-test (E)

Figure 2iv

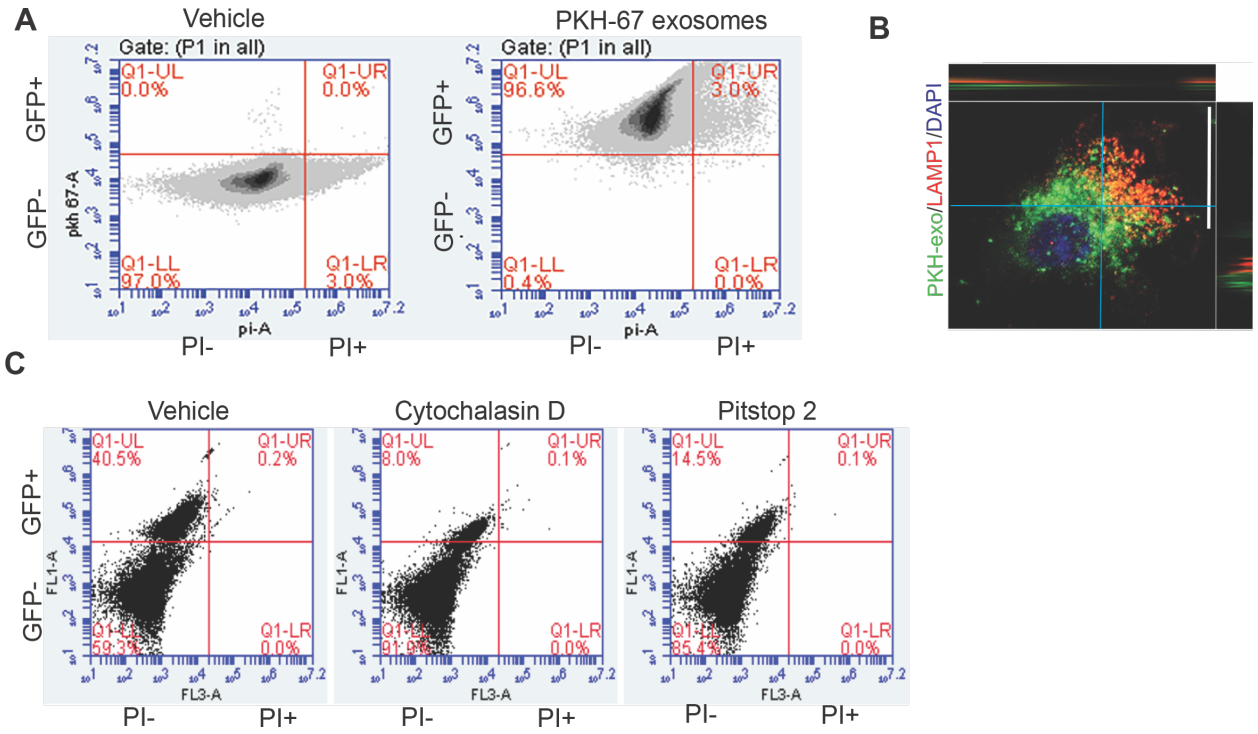

Figure 2.4: Microglia internalize exosomes via endocytic and phagocytic mechanisms

BV2 microglia were treated overnight with purified exosomes that were labeled with fluorescent dye, PKH 67, and analyzed wither by flow cytometry or microscopy. (A) Flow cytometry analysis showing green fluorescent signal in exosome- but not vehicle-treated microglia. (B) Representative confocal image of microglia treated with PKH-67 exosomes, showing perinuclear localization of exosomes with minimal lysosomal targeting (Scale bar = 10nm, red = LAMP1, green = PKH-exo). (C) Internalization of exosomes was further confirmed using assays performed in the presence of cytochalasin D or pitstop2. Reduced GFP signal (top left quadrant) in inhibitor compared to vehicle-treated BV2 microglia confirmed that microglia exosome internalization is dependent on actin polymerization and clathrin endocytosis.

Figure 2v

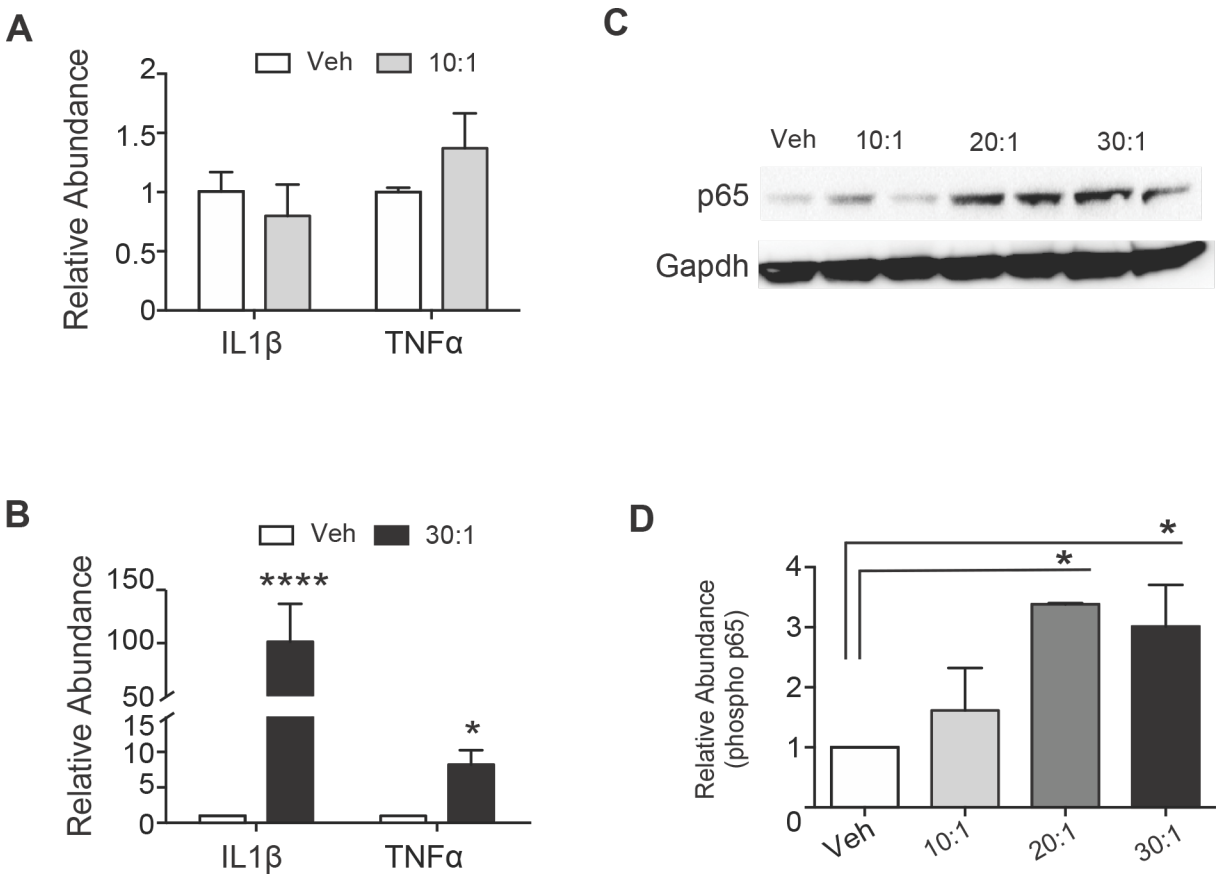

Figure 2.5: Exosome stimulation is sufficient to induce microglia inflammatory activation

Exosomes were collected from 10, 20 or 30 times as many producing microglia as recipient microglia, 10:1, 20:1 and 30:1 stimulation ratios, and then analyzed for gene expression. (A) Low ratio of exosome stimulation (10:1) did not result in significant changes in expression levels of *IL1β* and *TNFα.* (B) High ratio of exosome stimulation (30:1) resulted in significant upregulation of *IL1β* and *TNFα* transcript levels. (C) Western blot probes for NFκB, phospho-p65, and Gapdh in exosome stimulated microglia. (D) Quantification of phosphor p65 band intensity confirms dose dependent activation of microglia by exosomes. Data represented as mean ± SEM; **P*<0.05; *****P*<0.0001, t-test (A,B,D)

Figure 2vi

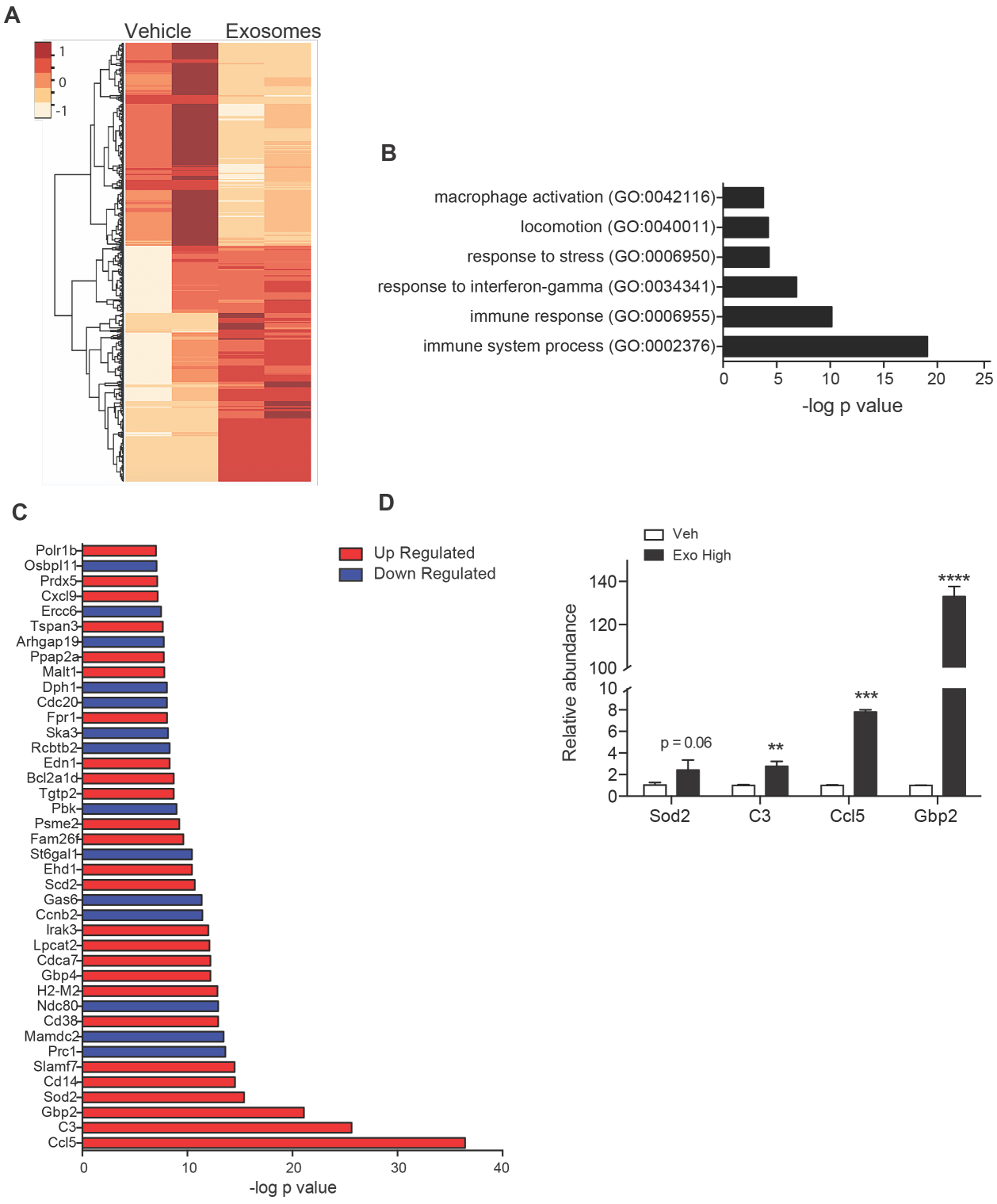
A
Vehicle
Exosomes
1
0
-1
B
macrophage activation (GO:0042116)
locomotion (GO:0040011)
response to stress (GO:0006950)
response to interferon-gamma (GO:0034341)
immune response (GO:0006955)
immune system process (GO:0002376)
0
5
10
15
20
25
-log p value
C
Up Regulated
Down Regulated
Polr1b
Osbpl11
Prdx5
Cxcl9
Ercc6
Tspan3
Arhgap19
Ppap2a
Malt1
Dph1
Cdc20
Fpr1
Ska3
Rcbtb2
Edn1
Bcl2a1d
Tgtp2
Pbk
Psme2
Fam26f
St6gal1
Ehd1
Scd2
Gas6
Ccnb2
Irak3
Lpcat2
Cdca7
Gbp4
H2-M2
Ndc80
Cd38
Mamdc2
Prc1
Slamf7
Cd14
Sod2
Gbp2
C3
Ccl5
0
10
20
30
40
-log p value
D
Veh
Exo High
Relative abundance
140
120
100
10
8
6
4
2
0
p = 0.06
**
***
****
Sod2
C3
Ccl5
Gbp2

Figure2.6: Transcriptome profile of exosome stimulated microglia showing activation of immune pathways, including interferon response genes

(A) Heatmap showing distribution of differentially expressed genes between IFNγ exosome-treated and vehicle-treated microglia as identified by RNA sequencing. (B) Panther overrepresentation analysis of differentially expressed genes identified gene ontology networks associated with immune response, response to interferon, gamma, macrophage activation (C) Top 40 differential expressed genes in IFNγ exosome-compared to vehicle-treated microglia, many of which are associated with inflammatory responses (red = upregulated, blue = downregulated). (D) qPCR validation of differentially expressed genes identified by RNAseq showing exosome induced upregulation of interferon genes (*Gbp2*) and immune effector molecules (*Ccl5* and *C3*). Data represented as Mean±SEM; ***P*<0.01, ****P*<0.001, *****P*<0.0001; Multiple t-test with Bonferroni correction (A,B), t-test (D).

Figure 2vii

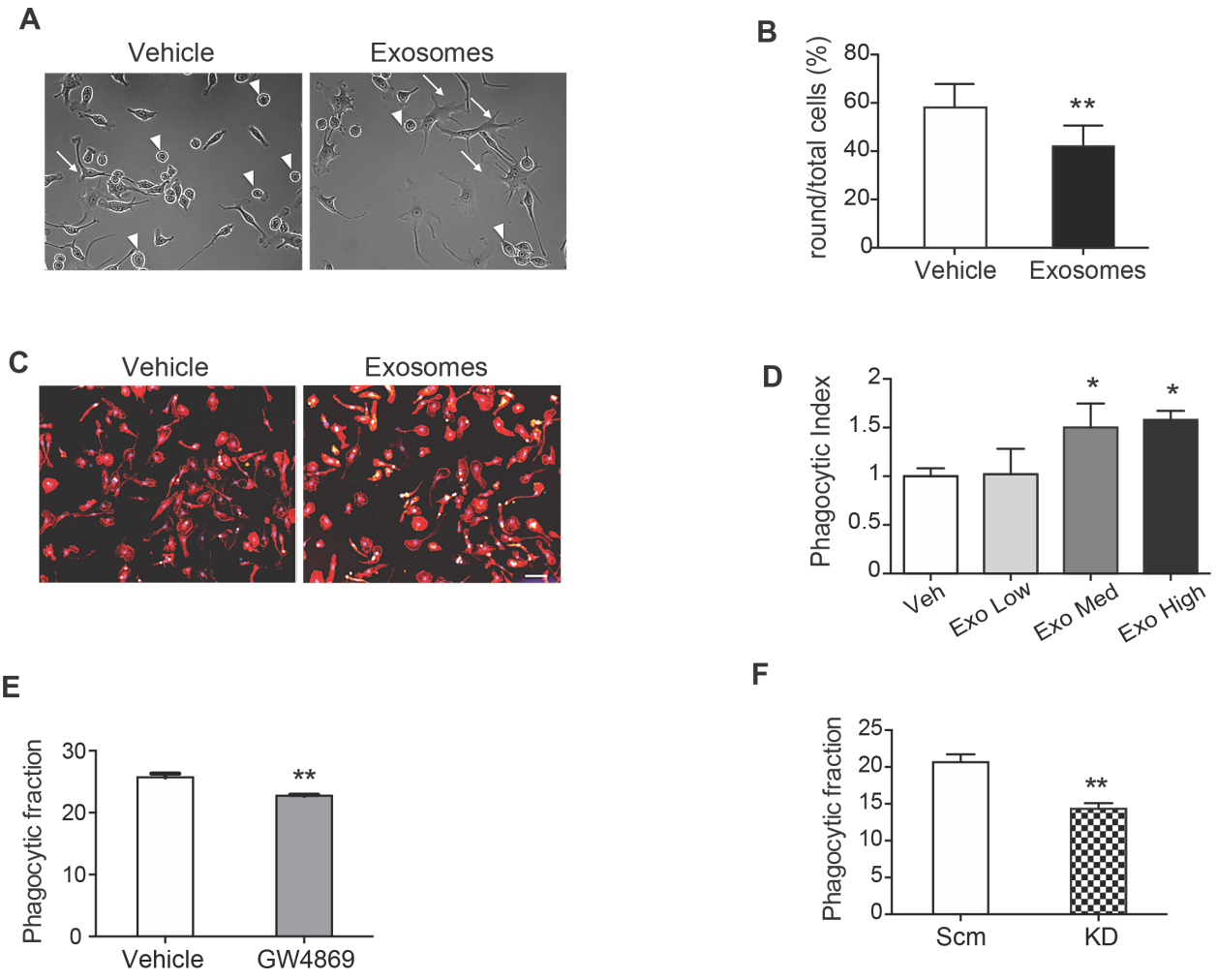

Figure 2.7 Exosomes are necessary for efficient microglia phagocytosis

(A) Representative micrographs obtained from live cell imaging of exosome- and vehicle-treated microglia showing microglia morphological changes in response to exosome stimulation (arrowheads – round, arrows – ramified, scale = 50μm). (B) Exosome stimulation resulted in altered microglia morphology, characterized by transformation increased morphology and significant reduction in the number of cells with round morphology per frame. (C) Representative images showing exosome- and vehicle-treated microglia treated with opsonized latex beads. (D) A dose-dependent

enhancement of bead uptake was observed in exosome- compared to vehicle-treated BV2 microglia and quantified as phagocytic index, i.e, total number of beads over total number of cells. (E,F) Reduced bead uptake in GW4969 treated and rab27a kd microglia compared to respective controls further confirmed the importance of exosomes in regulating microglia phagocytosis. Data represented as Mean±SEM; *P<0.05, **P<0.01; t-test (B,E,F); one-way ANOVA (D).

Figure 2viii

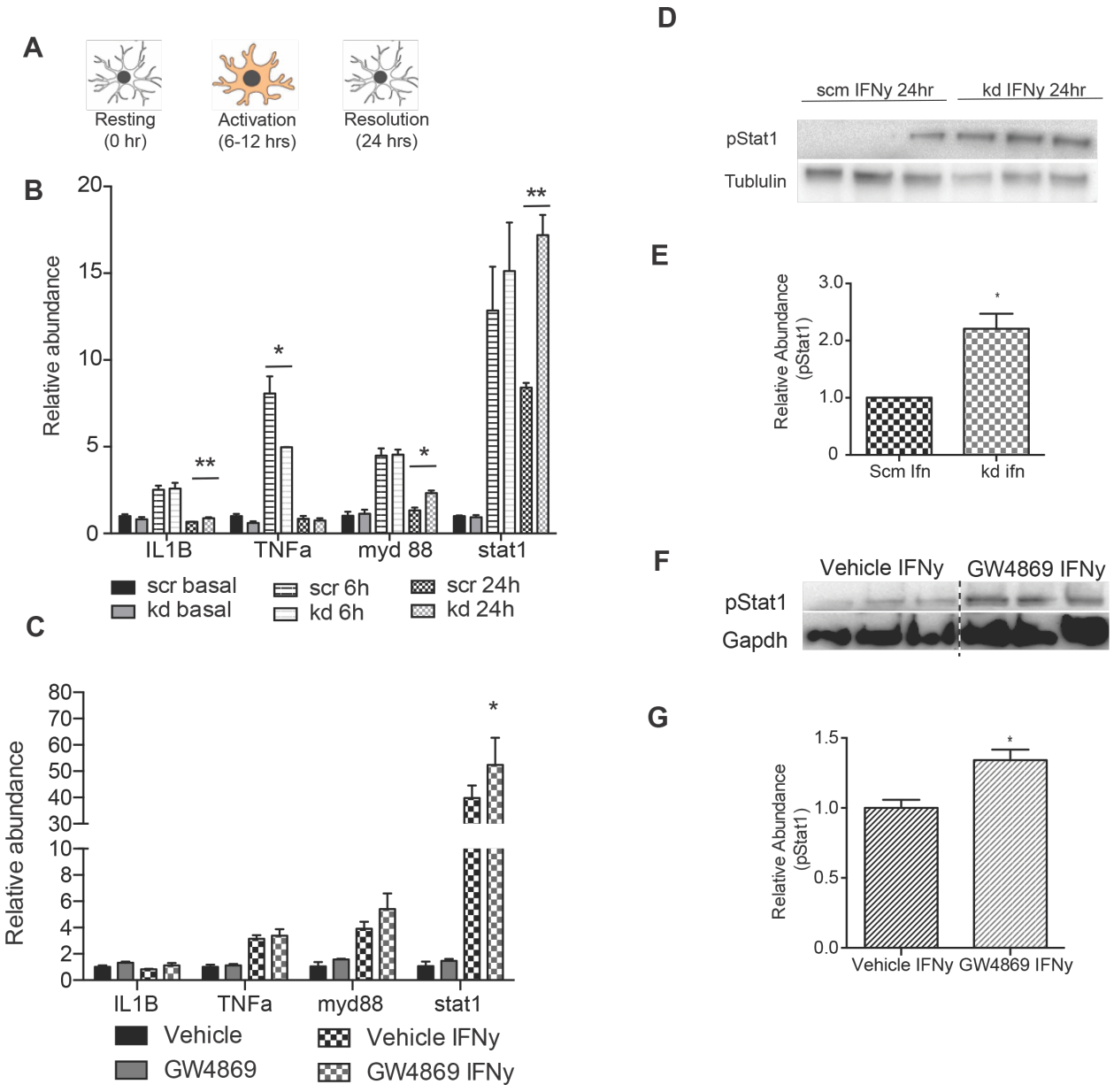

Figure 2.8 Impaired exosome production impairs inflammatory resolution in activated microglia

(A) Schematic showing classification of microglia status, into resting, activation, and resolution, based on time-dependent changes in inflammatory gene expression in response to IFNγ. (B) qPCR timecourse of unactivated and IFNγ activated (6 and 24 hrs)

BV2 microglia showing significant changes in the expression profiles of proinflammatory cytokines, *IL1β* and *TNF IL1β,* and inflammatory signaling molecules, *myd88* and *stat1* in rab27 kd compared to scm microglia. (C) qPCR analysis of unactivated and IFNγ activated microglia showing increased *Stat1* expression in GW4869 cells compared to controls. (D) Western blot analysis of IFNγ activated scm and kd microglia probed for phosphorylated Stat1 and tubulin. (E) Stat1 phosphorylation is significantly increased in kd compared to scm microglia. (F) Western blot analysis of IFNγ activated GW4869 or vehicle treated microglia probed for phosphorylated Stat1 and Gapdh. (G) Stat1 phosphorylation is significantly increased in GW4869 compared to vehicle treated microglia. Data represented as mean ± SEM; **P*<0.05; ***P*<0.01; t-test (B,C,E,G).

Figure 2ix

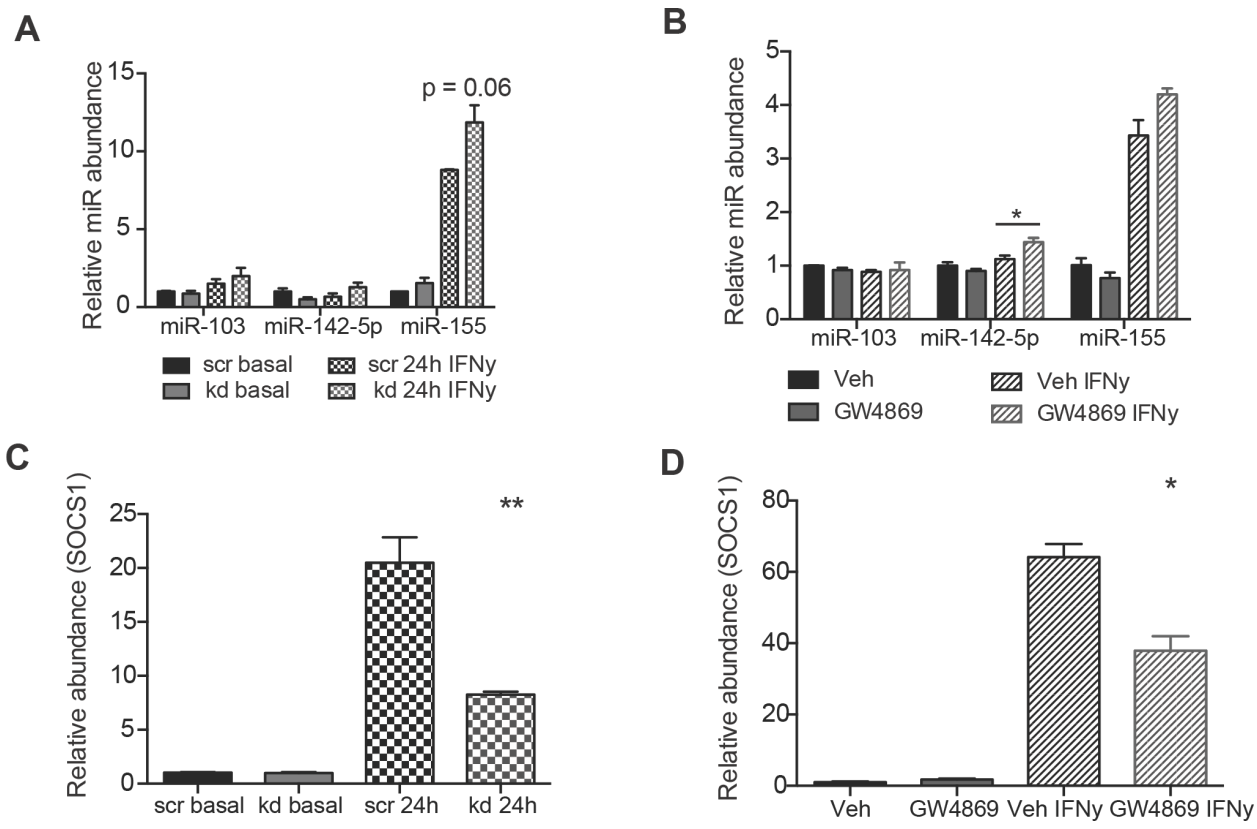

Figure 2.9: Impaired miR-155 microRNA trafficking in exosome impaired microglia results increased targets repression

(A,B) qPCR analyses of IFNγ exosome enriched miRNAs showing increased cellular abundance in rab27a kd and GW4869 treated BV2 microglia compared to respective scm and vehicle treated controls. (C,D) Increased miR-155 expression in rab27a kd and GW4869 treated microglia corresponds with decreased expression of SOCS1, a miR-155 target and important suppressor of IFNγ mediated inflammation. Data represented as mean ± SEM; **P*<0.05; ***P*<0.01; t-test (A-D).

Figure 2x

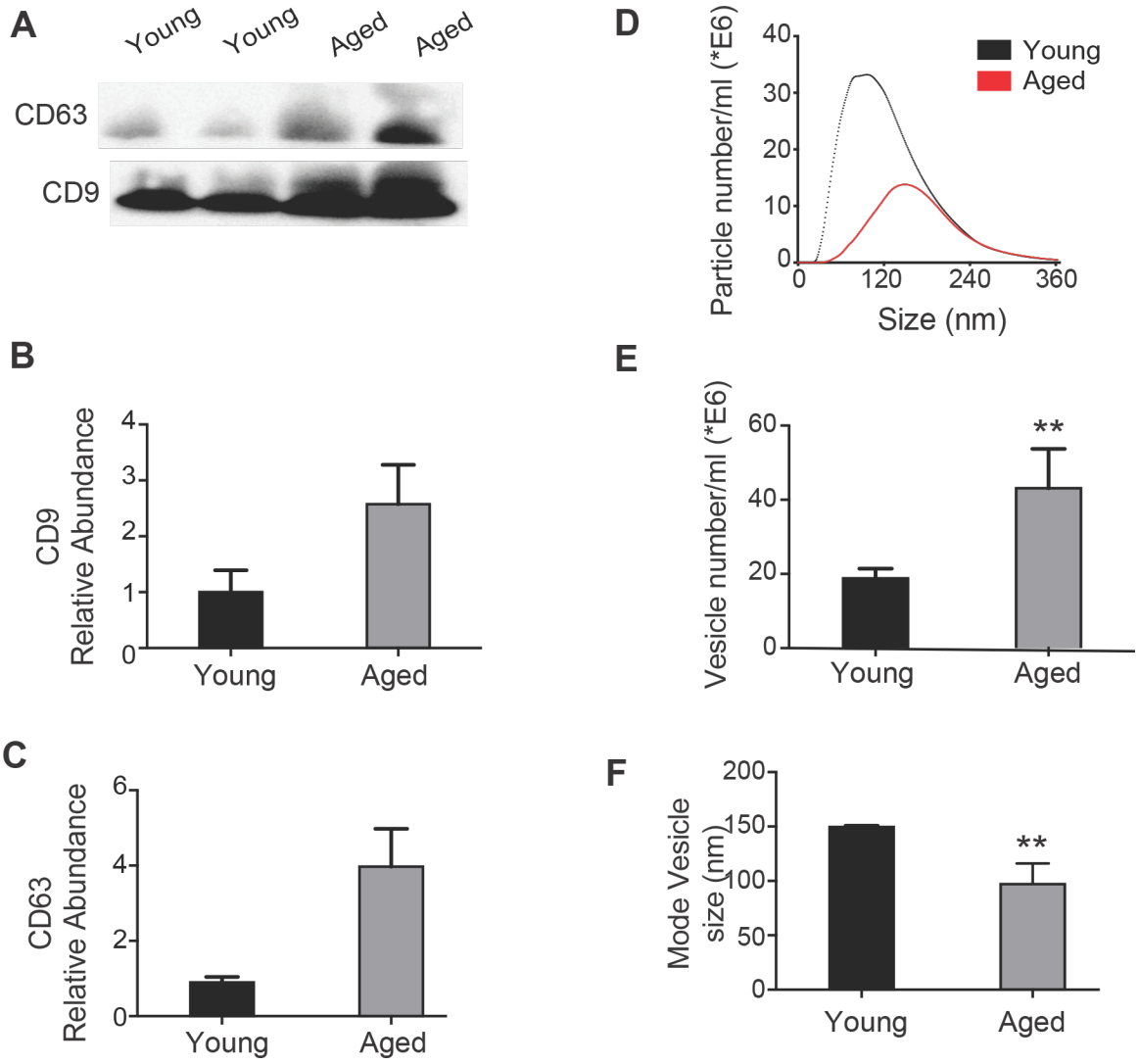

Figure 2.10: Brain aging results in increased abundance of interstitial exosomes

(A) Representative western blot probes for tetraspanin protiens, CD9 and CD63, in exosomes isolated from young (3 months) and aged (18 months) hemibrains. (C,D) Western blot quantification showing higher CD9 and CD63 expression in aged compared young brain exosomes. (E) Representative nanoparticle tracking traces of young and aged brain exosomes. (F,G) Aged brains contain significantly more interstitial exosomes,

characterized by reduced mode vesicle size compared to exosomes from young brains. Data represented as mean ± SEM; *P<0.05; **P<0.01; t-test (B,C,E,F).

Figure 2xi

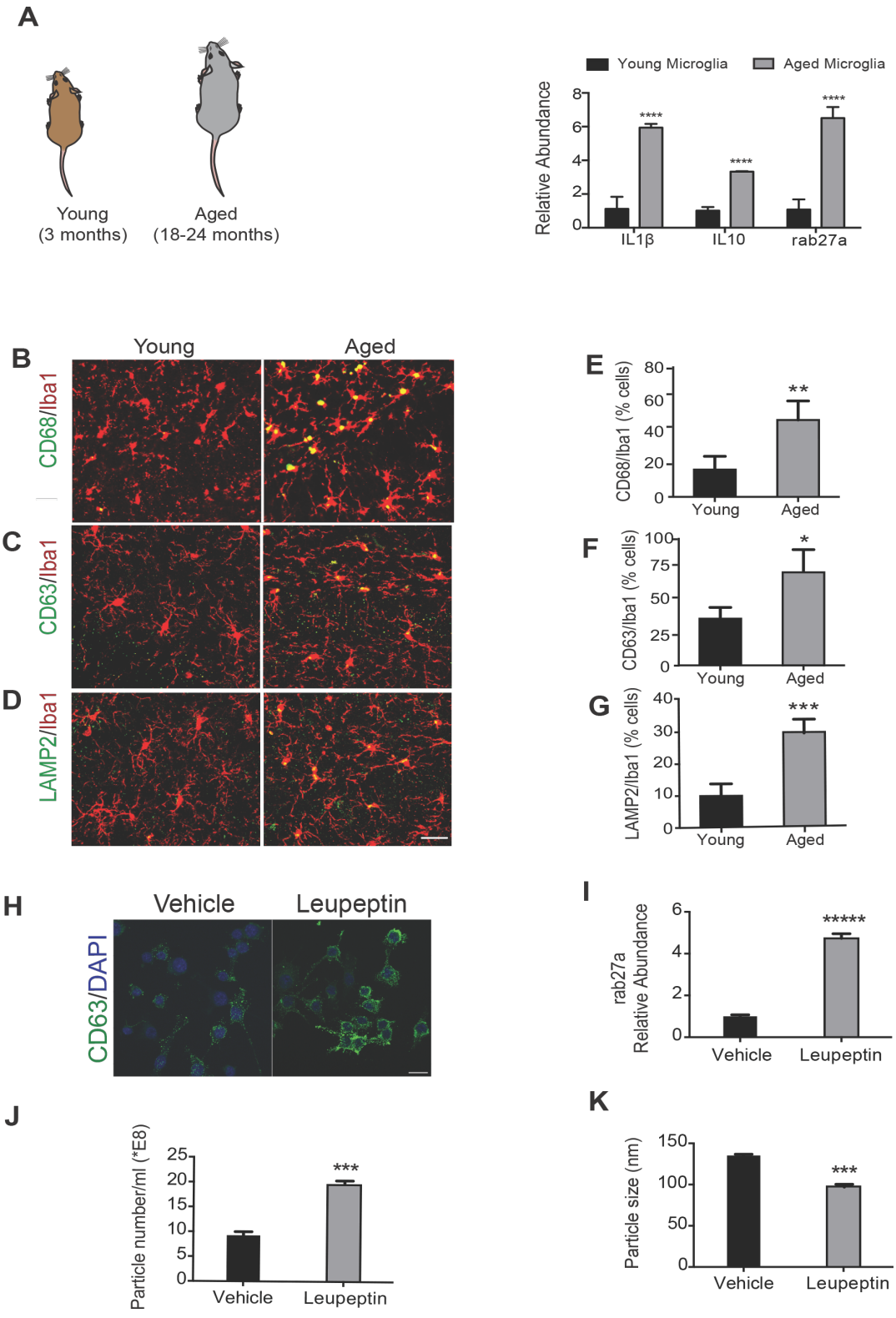
A
Young
(3 months)
Aged
(18-24 months)
Young Microglia
Aged Microglia
Relative Abundance
IL1β
IL10
rab27a
B
Young
Aged
CD68/Iba1
C
CD63/Iba1
D
LAMP2/Iba1
E
CD68/Iba1 (% cells)
F
CD63/Iba1 (% cells)
G
LAMP2/Iba1 (% cells)
H
Vehicle
Leupeptin
CD63/DAPI
I
rab27a
Relative Abundance
J
Particle number/ml (*E8)
K
Particle size (nm)

Figure 2.11: Aging associated increase in microglia *rab27a* expression is partially driven by lysosomal dysfunction

(A) qPCR analysis of acutely isolated microglia from young (3 month) and aged mice (24 month) showing increased expression of inflammatory genes, *IL1β* and *IL4,* as well as exosome regulatory gene, *rab27a*. (B-D) Representative fluorescent images of young and aged microglia (Iba1, red) showing expression of patterns of endolysosomal and exosome associated proteins, CD68, CD63, and LAMP2 (green). (E-G) Aged microglia express significantly higher levels of CD68, CD63 and LAMP2 than young microglia (n = 5 per group). (H,I) Inhibition of lysosome proteolytic function *in vitro* by leupeptin treatment is sufficient to alter CD63 expression and increase *rab27a* expression. (J,K) Leupeptin treated microglia produce significantly more exosomes with reduced mode vesicle size, similar to aged microglia. Data represented as Mean±SEM; **P*<0.05, ***P*<0.01; ****P*<0.001; *****P*<0.0001; t-test (B, E-G, I-K).

Figure 2xii

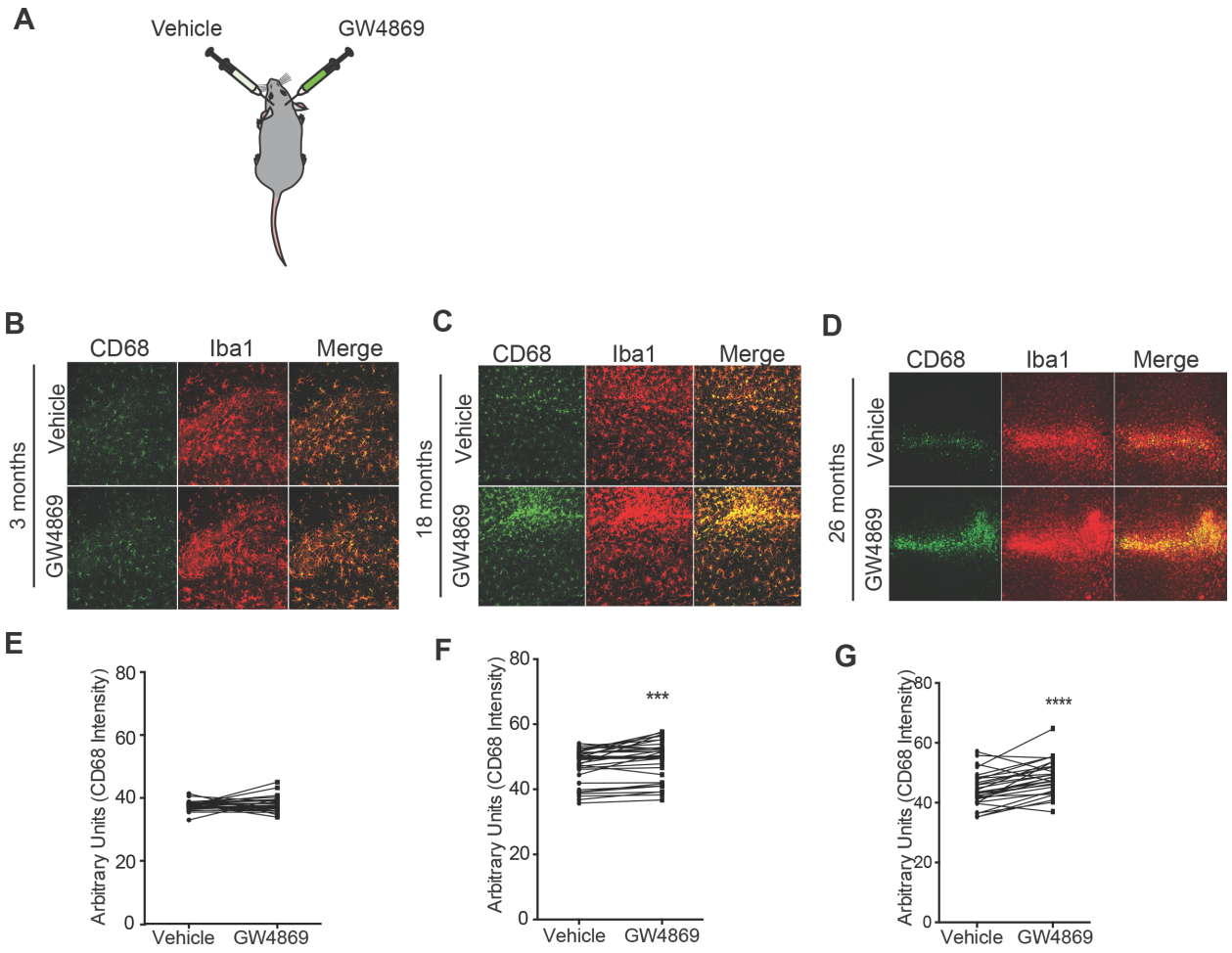

Figure 2.12: Inhibition of exosome production results in increased microglia activation in aged and old brains

(A) Schematic demonstrating method for local inhibition of exosomes in the brain via unilateral stereotaxic injections of GW4869 or vehicle. (B-E) Representative immunofluorescent images of vehicle and GW4869 injected hemibrains stained for microglia marker, Iba1, and activation marker, Cd68. (F-H) Quantification of CD68 intensity in the injected brain regions showing an age dependent effect of blocking exosomes on microglia activation. GW4869 injection resulted in increased CD68

expression only in aged microglia (18 and 24 months) and not in young microglia (3 month). Data represented as Mean±SEM; $^{**}P < 0.01$; $^{***}P < 0.001$, paired t-test (F-H).

Figure 2xiii

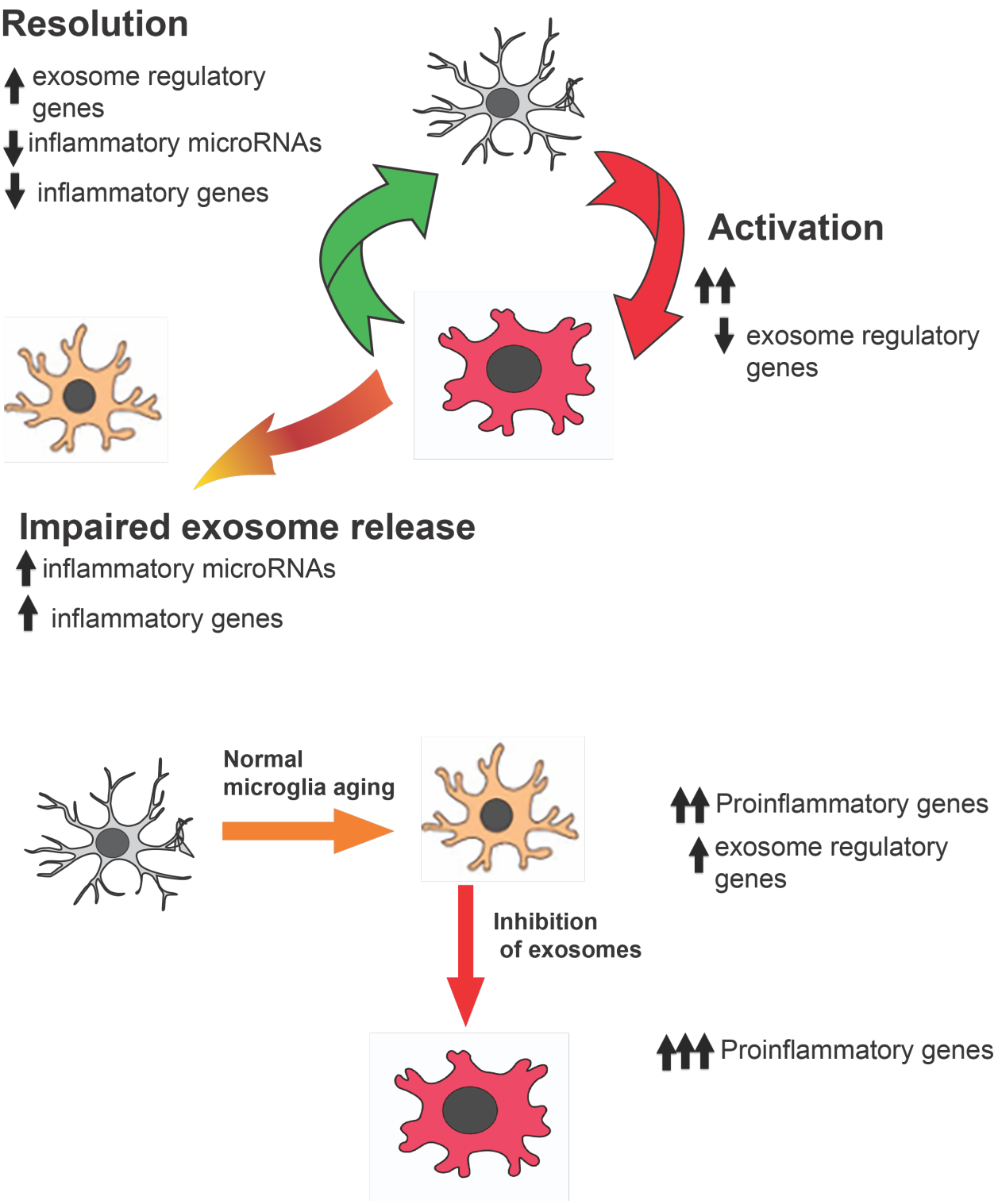

Figure 2.13: Models demonstrating exosome mediated regulation of acutely and chronically activated microglia. (A) In acutely activated microglia, increased expression

of pro-inflammatory genes (*Il1β*, *TNFα,* and *stat1*) is accompanied by reduced expression of exosome regulatory genes (*nSMase2* and *rab27a*) while induction of exosome regulatory genes promotes resolution of activation via release of immune microRNAs such as miR-155. (B) In the aging brain, activated microglia express higher levels of both inflammatory and exosome regulatory genes. Blockage of exosome release results in exacerbation of activation, indicated by increased CD68 expression.

Table 2.1

IFNγ Activated microglia exosomes			Unactivated microglia exosomes		
Y1-001727	mmu-miR-383	mmu-miR-15b	Y1-001727	mmu-miR-337-5p	mmu-miR-129-3p
snoRNA202	mmu-miR-380-5p	mmu-miR-15a	snoRNA202	mmu-miR-335-5p	mmu-miR-128a6
rno-miR-760-5p	mmu-miR-376c	mmu-miR-155	snoRNA135	mmu-miR-331-3p	mmu-miR-127
rno-miR-532-5p	mmu-miR-376a	mmu-miR-153	rno-miR-760-5p	mmu-miR-328	mmu-miR-126-5p
rno-miR-381	mmu-miR-365	mmu-miR-152	rno-miR-381	mmu-miR-324-5p	mmu-miR-126-3p
rno-miR-351	mmu-miR-362-3p	mmu-miR-151-3p	rno-miR-351	mmu-miR-324-3p	mmu-miR-125b-5p
rno-miR-345-3p	mmu-miR-361	mmu-miR-150	rno-miR-224	mmu-miR-320	mmu-miR-125a-5p
rno-miR-224	mmu-miR-350	mmu-miR-146b	rno-miR-207	mmu-miR-30e	mmu-miR-125a-3p
rno-miR-207	mmu-miR-34a	mmu-miR-146a	rno-miR-190b	mmu-miR-30d	mmu-miR-10a
rno-miR-196c	mmu-miR-345-5p	mmu-miR-145	mmu-miR-99b	mmu-miR-30c	mmu-miR-106b
rno-miR-190b	mmu-miR-342-5p	mmu-miR-142-3p	mmu-miR-93	mmu-miR-30b	mmu-miR-106a
mmu-miR-99a	mmu-miR-342-3p	mmu-miR-141	mmu-miR-92a	mmu-miR-30a	mmu-miR-103
mmu-miR-93	mmu-miR-340-5p	mmu-miR-140	mmu-miR-9	mmu-miR-301b	mmu-miR-101a
mmu-miR-92a	mmu-miR-340-3p	mmu-miR-139-5p	mmu-miR-872	mmu-miR-301a	mmu-miR-100
mmu-miR-9	mmu-miR-339-3p	mmu-miR-138	mmu-miR-7b	mmu-miR-29c	mmu-let-7i
mmu-miR-872	mmu-miR-337-5p	mmu-miR-137	mmu-miR-7a	mmu-miR-29a	mmu-let-7g
mmu-miR-7b	mmu-miR-331-3p	mmu-miR-136	mmu-miR-744	mmu-miR-296-5p	mmu-let-7e
mmu-miR-7a	mmu-miR-328	mmu-miR-133a	mmu-miR-708	mmu-miR-28	mmu-let-7d
mmu-miR-744	mmu-miR-324-5p	mmu-miR-132	mmu-miR-685	mmu-miR-27b	mmu-let-7c
mmu-miR-685	mmu-miR-324-3p	mmu-miR-130b	mmu-miR-652	mmu-miR-27a	mmu-let-7b
mmu-miR-674	mmu-miR-320	mmu-miR-130a	mmu-miR-574-3p	mmu-miR-26b	
mmu-miR-671-3p	mmu-miR-31	mmu-miR-129-3p	mmu-miR-544	mmu-miR-26a	
mmu-miR-670	mmu-miR-30e	mmu-miR-128a	mmu-miR-532-5p	mmu-miR-25	
mmu-miR-669a	mmu-miR-30d	mmu-miR-127	mmu-miR-532-3p	mmu-miR-24	
mmu-miR-666-5p	mmu-miR-30c	mmu-miR-126-5p	mmu-miR-500	mmu-miR-224	
mmu-miR-652	mmu-miR-30b	mmu-miR-126-3p	mmu-miR-494	mmu-miR-223	
mmu-miR-598	mmu-miR-30a	mmu-miR-125b-5p	mmu-miR-484	mmu-miR-222	
mmu-miR-574-3p	mmu-miR-301b	mmu-miR-125a-5p	mmu-miR-467c	mmu-miR-218	
mmu-miR-544	mmu-miR-301a	mmu-miR-125a-3p	mmu-miR-467a	mmu-miR-210	
mmu-miR-539	mmu-miR-29c	mmu-miR-10a	mmu-miR-465a-5p	mmu-miR-21	
mmu-miR-532-5p	mmu-miR-29b	mmu-miR-106b	mmu-miR-434-3p	mmu-miR-20b	

mmu-miR-532-3p	mmu-miR-29a	mmu-miR-106a	mmu-miR-411	mmu-miR-20a
mmu-miR-500	mmu-miR-293	mmu-miR-101a	mmu-miR-384-3p	mmu-miR-204
mmu-miR-494	mmu-miR-28	mmu-miR-100	mmu-miR-379	mmu-miR-203
mmu-miR-484	mmu-miR-27b	mmu-miR-1	mmu-miR-376a	mmu-miR-200b
mmu-miR-467e	mmu-miR-27a	mmu-let-7i	mmu-miR-365	mmu-miR-19b
mmu-miR-467c	mmu-miR-26b	mmu-let-7g	mmu-miR-34b-3p	mmu-miR-19a
mmu-miR-467a	mmu-miR-26a	mmu-let-7e	mmu-miR-345-5p	mmu-miR-199a-5p
mmu-miR-465a-3p	mmu-miR-25	mmu-let-7d	mmu-miR-342-3p	mmu-miR-199a-3p
mmu-miR-434-3p	mmu-miR-24	mmu-let-7c	mmu-miR-340-5p	mmu-miR-197
mmu-miR-384-5p	mmu-miR-23b		mmu-miR-339-3p	mmu-miR-195
mmu-miR-224	mmu-miR-196b		mmu-miR-193b	mmu-miR-150
mmu-miR-223	mmu-miR-195		mmu-miR-193	mmu-miR-148b
mmu-miR-222	mmu-miR-193b		mmu-miR-192	mmu-miR-146b
mmu-miR-218	mmu-miR-193		mmu-miR-191	mmu-miR-146a
mmu-miR-215	mmu-miR-192		mmu-miR-18a	mmu-miR-145
mmu-miR-210	mmu-miR-191		mmu-miR-188-5p	mmu-miR-142-5p
mmu-miR-21	mmu-miR-18a		mmu-miR-186	mmu-miR-142-3p
mmu-miR-20b	mmu-miR-188-5p		mmu-miR-184	mmu-miR-140
mmu-miR-20a	mmu-miR-186		mmu-miR-183	mmu-miR-139-5p
mmu-miR-204	mmu-miR-184		mmu-miR-182	mmu-miR-138
mmu-miR-203	mmu-miR-183		mmu-miR-181a	mmu-miR-137
mmu-miR-200b	mmu-miR-182		mmu-miR-17	mmu-miR-135b
mmu-miR-19b	mmu-miR-181c		mmu-miR-16	mmu-miR-133a
mmu-miR-19a	mmu-miR-181a		mmu-miR-15b	mmu-miR-132
mmu-miR-199a-3p	mmu-miR-17		mmu-miR-15a	mmu-miR-130b
mmu-miR-197	mmu-miR-16		mmu-miR-155	mmu-miR-130a

Table 2.1 Summary of BV2 microglia exosomal microRNA composition

List of all miRNAs identified by Taqman miRNA expression assay in IFNγ activated and unactivated BV2 microglia exosomes

Table 2.2

Shared proteins			Unactivated		IFNγ Activated	
Afm	Hist1h2ak	Rac3	Acox3	Spp1	Actg1	Rab1A
Ahsg	Hist1h2bb	Ran	Acta1	Tpi1	Alcam	Rab1b
Alb	Hist1h2bc	Rap1a	Actb	Tubb3	Anxa3	Rab7a
Aldoa	Hist1h2bf	Rpl14	Actc1	Tubb6	Anxa5	Rhoa
Alpl	Hist1h2bh	Rpl18	Anp32b	Sh3gl2	Apoh	Rpl11
Anpep	Hist1h2bk	Rpl30	Arhgdia		Atp1b3	Rpl13
Anxa2	Hist1h2bm	Rpl7	Aprt		B2m	Rpl3
Anxa4	Hist1h2bp	Rps11	Arf1		Btd	Rpl5
Apoe	Hist1h4a	Rps18	Arf2		Cd28	Rpl7a
Atp1a1	Hist2h2aa1	Rps3	Arf3		Cd81	Rplp0
Atrn	Hist2h2ab	Rps4x	Arhgdia		Cd9	Rps14
Basp1	Hist2h2ac	Rps5	Arl8a		Cfl1	Rps15a
Bsg	Hist2h2bb	Rps8	Arl8b		Clic1	Rps16
Cd44	Hist2h2be	Rpsa	C1ra		Cndp1	Rps17
Cdc42	Hist3h2a	Scamp3	C1rb		Dnah3	Rps13
Cdh13	Hist3h2ba	Sdcbp	C1rl		Eci1	Rps2
Chmp4b	Hist3h2bb	Serping1	Cep104		Ehd4	Rps23
Clta	Hp	Slc16a1	Ctsd		Eif4a1	Rps26
Cltc	Hpx	Slc38a2	Cp		Eif4a2	Rps27
Clu	Hsp90aa1	Slc3a2	Dip2b		Emb	Rps27a
Eef1a1	Hsp90ab1	Slc7a5	Gnb4		Emr1	Rps27l
Eef1g	Igsf8	Smpdl3b	Hbb-y		F10	Rps7
Eno1	Itga4	Tf	Heph		Fabp5	Rps9
Fcer1g	Itgb1	Tfrc	Hic2		Fermt3	Sdc4
Fignl1	Itgb2	Tuba1a	Hist1h2ba		Gnb2l1	Serpinf1
Gapdh	Lpl	Tuba1b	Hspa8		Gpnmb	Sirpa
Glipr2	Lum	Tubb4a	Ilk		Hspa4	Slc1a5
Gnai2	M6pr	Tubb4b	Marveld2		Hspa4l	Tex101
Gnb1	Mfge8	Tubb5	Pcbp1		Hspa8	Tjp3
Gnb2	Mif	Uba52	Pcbp2		Hsph1	Tpi1
Grn	Mrc1	Ubb	Pcbp3		Itgam	Tspan4
H2afj	Mvp	Ubc	Pdxp		Lcat	Ywhae
H2afv	Pdcd6ip	Vat1	Rac2		Ldha	Ywhaz
H2afx	Pfn1	Vim	Rap1b		Lgals3	Hic2
H2afz	Pgk1	Vps28	Rhog		Msn	
Hba	Pglyrp2	Vps4a	Rhoq		Pabpc1	
Hbb-b1	Phgdh	Vps4b	Rpl12		Pepd	

Hbb-b2	Pkm		Rpl24		Pidd1	
Hist1h2ab	Ppia		Rps27a		Plek	
Hist1h2af	Prdx1		Rpl9		Psat1	
Hist1h2ah	Rac1		Sh3gl1		Rab10	

Table 2.2: Exosomal proteins identified in unactivated and activated BV2 microglia

List of proteins found in BV2 microglia exosomes identified by mass spectrometry.

CHAPTER 3
DICER REGULATES ADULT MICROGLIA HOMEOSTASIS AND FUNCTION IN THE HIPPOCAMPAL STEM CELL NICHE

3.1 ABSTRACT

MicroRNAs (miRNAs) are important post-transcriptional regulators of gene expression involved in developmental specification, cellular identity and tuning of physiological responses[46,68,70]. Various studies, including ours above, have highlighted the involvement of miRNAs in regulation of peripheral and central immune responses[71,72]. While there exists abundance of evidence supporting miRNA regulation of microglia inflammation in disease[73,74], not much is known about miRNA function in microglia in the adult non-diseased brain. Here, we utilize tamoxifen induced deletion of miRNA processing enzyme, Dicer, to investigate the roles of miRNAs in adult microglia function. Deletion of dicer adversely affects various microglia properties including survival, morphology and inflammation. Additionally, we observe a significant alteration of hippocampal stem cell number in the brains of mice with depleted adult microglia dicer. Our findings highlight the involvement of dicer-dependent miRNA production in broad regulation of adult microglia physiology, with important consequences on brain homeostasis. Thus, this study expands on the current view of adult microglia homeostatic functions to include miRNA-dependent regulations and also reveals new miRNA-dependent mechanisms of regulating the hippocampal stem cell niche.

3.2 RESULTS

3.2.i Dicer depletion in adult microglia results in impaired survival and altered morphology

To investigate the functions of dicer in adult microglia *in vivo,* we generated an inducible model by crossing CX3cr1^{CreER} mice with Dicer$^{fl/fl}$ mice, and subsequently crossing the F1

progenies[75]. Resultant Cx3cr1^{CreER} Dicer$^{fl/fl}$ (Cre^{+}) and Dicer$^{fl/fl}$ or Cx3cr1^{CreER} Dicer$^{+/+}$ (Cre^{-}) littermates were injected with tamoxifen (TAM) at 6-8 weeks of age and consequences of dicer depletion were investigated 8 weeks post injections. This time point of analysis was chosen to allow turnover of other myeloid cell and tissue macrophage populations, thus restricting dicer depletion to microglia specifically[76]. PCR analysis of brain tissue collected from TAM-injected animals confirmed the expression of the recombined dicer allele only in Cx3cr1^{CreER} Dicer$^{fl/fl}$ animals, not in controls (Figure 3.1A). To further confirm recombination, expression of exon III of the *dicer* gene, which is flanked by flox sites in Dicer$^{fl/fl}$ mice[77], was assessed in microglia isolated from TAM-injected Cre^{+} and Cre^{-} mice. Indeed, expression of *dicer* exon III was significantly lower in Cx3cr1^{CreER} Dicer$^{fl/fl}$ microglia compared to controls (Figure 3.1B). These results confirm effective TAM-induced recombination thus validating our model for dicer depletion in adult microglia.

Next, we investigated the effects of dicer depletion on microglia. qPCR analysis of hemibrains collected 8 weeks post-TAM injection, revealed significantly reduced expression of colony stimulating factor receptor 1 (*Csfr1*) and transforming growth factor beta receptor 2 (*Tgfbr2*) in Cx3cr1^{CreER} Dicer$^{fl/fl}$ hippocampal lysates compared to controls (Figure 3.1C). In line with previous studies showing *Csf1r* and *Tgfbr2* as important regulators of microglia survival[7,78], we observed significantly reduced Iba1 immunoreactivity in Cx3cr1^{CreER} Dicer$^{fl/fl}$ brains compared to controls (Figure 3.1D,E). Quantification of microglia cell number in the hippocampi and cortices of in TAM-injected Cx3cr1^{CreER} Dicer$^{fl/fl}$ brains confirmed significantly fewer Iba1^{+} cells compared to controls

(Figure 3.1F,G). These observations support a novel role for dicer-dependent miRNA production in the regulation of adult microglia survival, as recently suggested[66].

We next asked if dicer depletion also impacted adult microglia morphology. Microglia morphology was assessed using Sholl analyses, which measures the extent of branching based on process intersection of concentric circles around a defined cell area (Figure 3.2A). Although dicer depletion did not impact microglia ramification index, Cx3cr1^{CreER} Dicer$^{fl/fl}$ microglia showed consistent morphological alterations characterized by increased number of branches, process length, and sum of intersections compared to controls (Fig 3.2 C-D). These changes imply that although microglia ramification is not grossly reorganized, dicer-depletion is associated with a greater degree of process extension compared to control microglia. This phenotype is likely due in part to increased surveillance burden placed on the microglia in TAM-injected Cx3cr1^{CreER} Dicer$^{fl/fl}$ mice compared to controls. Taken together, our findings show that dicer is critical for microglia homeostasis through regulation of viability and process extension.

3.2.ii Dicer-depleted microglia exhibit an aberrant inflammatory signature

To more broadly assess the effects of dicer depletion on adult microglia, we performed global transcription analysis by high throughput RNA sequencing of acutely isolated TAM-injected Cx3cr1^{CreER} Dicer$^{fl/fl}$ and control microglia. Over 600 genes were differentially expressed in dicer-depleted microglia compared to controls, with most showing downregulated expression compared to control (Figure 3.3A). Among the top differentially expressed genes, we consistently observed genes involved in inflammation, such as *S100a9*, *Fcer1g*, and *Ifngr1*, as well as genes involved in endolysosomal function such

as *Lamp1* and *Cstz* (Figure 3.3B). To better understand the biological consequences of dicer depletion in adult microglia, we performed gene set enrichment analyses (GSEA) on the differentially expressed genes identified by RNA sequencing (Figure 3.3 C,D). Given the broad nature of miRNA dependent regulation of gene expression, we expectedly found many gene signatures overrepresented in our list. As predicted by data above, we found genes involved in survival, mTORC1 signaling and apoptosis. Intriguingly, GSEA revealed a strong dysregulation of inflammatory pathways; more than half of GSEA pathways in downregulated genes are directly involved in inflammatory signaling (Figure 3.3D).

To directly assess the consequence of these observed transcriptional changes in microglia, we asked if microglia activation was altered in dicer depleted microglia. qPCR analyses revealed significant changes in expression of proinflammatory cytokine gene, *IL1B*, and microglia identity gene, *Sall1*, in dicer depleted compared to control microglia (Figure 3.4A). The observed increase in *IL1B* and decrease in *Sall1,* are in line with more proinflammatory activation signature based on previous studies[79]. To confirm this observation, we performed immunofluorescence labeling of microglia activation marker, CD68, of Cx3cr1^{CreER} Dicer$^{fl/fl}$ and control brains (Figure 3.4B). In line with the qPCR data, we observed significantly higher number of CD68^{+} microglia in Cx3cr1^{CreER} Dicer$^{fl/fl}$ compared to control brains (Figure 3.4C). Interestingly, this observed proinflammatory state does not result in transformation to an amoeboid morphology according to the classical paradigm of microglia activation. This is possibly due to the dysregulation of other inflammatory signaling pathways and downstream effectors in dicer depleted microglia as suggested by GSEA above. Moreover, it points to distinct regulatory

mechanisms driving upregulation of proinflammatory genes and morphological transformation in adult microglia and lends support to the notion that microglia activation exists in a continuum[80]. More work is needed to identify mechanistic drivers of this observed decoupling of microglia activation and morphology. Notwithstanding, we provide evidence for the involvement of dicer in promoting maintenance of a low inflammatory profile in adult microglia.

3.2.iii Microglia dicer deficiency alters the cellular composition of the hippocampal stem cell niche

Given the observed aberrant inflammatory activation of dicer depleted microglia, we next asked its impact on other brains cells. We focus here on the hippocampus – an area of the brain that is highly susceptible to inflammation induced dysfunction[81]. To assess the effects of microglia dicer depletion of hippocampal stem cells, we stained TAM-injected Cx3cr1^{CreER} Dicer$^{fl/fl}$ and control brains for markers of different stages of neural stem cell differentiation, namely nestin, MCM2 and doublecortin to label neural stem cells, neuronal progenitors, and immature neurons, respectively[82] (Figure 3.5A). Dicer depletion in microglia had an overall inhibitory effect on all stages of hippocampal neurogenesis, based on reduced cell numbers in TAM-injected Cx3cr1^{CreER} Dicer$^{fl/fl}$ DG compared to controls (Figure 3.5B). However, cell numbers were significantly different only for neuronal progenitor (MCM2^{+}) and immature neurons (DCX^{+}), Cx3cr1^{CreER} Dicer$^{fl/fl}$ hippocampi containing significantly fewer cells compared to controls (Figure 3.5B). To better understand the transition of cells between these several development stages, we performed lineage progression analysis by dividing the number of cells in a particular

stage with the number of cells in the preceding stage. Comparison of lineage progression revealed significant differences in neural stem cells to neuronal progenitor transition (Nestin/MCM2) but not in neuronal progenitor to immature neuron transition (MCM2/DCX) (Figure 3.5C). This observation points to microglia dicer depletion significantly altering neural stem cell differentiation not stem cell maturation. Neural stem cells have the ability to give rise to both neuronal and astrocytic progenitors. We next asked if there was evidence of altered astrocyte formation in the granule cell layer of the hippocampi of $Cx3cr1^{CreER}$ $Dicer^{fl/fl}$ and control brains by staining for astrocyte marker glia fibrillary acidic protein (GFAP) (Figure 3.5D). Analyses of GFAP intensity revealed increased intensity in the granule cell layer of $Cx3cr1^{CreER}$ $Dicer^{fl/fl}$ compared to hippocampi (Figure 3.5E). Our findings identify dicer function in microglia as an important extrinsic mechanism for maintaining the adult stem cell maintenance niche, via regulation of neural stem cell differentiation. We provide preliminary evidence suggesting that dicer-mediated microglia responses can skew neural stem cell lineage commitment. Future studies are necessary to tease out the nature of this regulation and miRNAs and signaling molecules involved.

3.2.iv Microglia dicer deficiency does not elicit broad changes in hippocampal-dependent behavior

Given the cellular changes observed in the $Cx3cr1^{CreER}$ $Dicer^{fl/fl}$ dentate gyrus, we next asked if these changes altered hippocampal dependent learning and behavior. We used contextual fear conditioning and radial arm water maze (RAWM) paradigms to test hippocampal dependent learning and memory in $Cx3cr1^{CreER}$ $Dicer^{fl/fl}$ mice and control litter mates (Figure 3.6A). Overall, $Cx3cr1^{CreER}$ $Dicer^{fl/fl}$ and control mice learned the

location of the platform in the RAWM and were able to recall this location during hidden platform tests (Figure 3.6B-D). Interestingly, control mice showed slightly better learning than Cx3cr1^{CreER} Dicer$^{fl/fl}$ mice when number of errors in the training day (block 1) are compared to errors in testing day 2 (block 3) (Figure 3.6D). However, we failed to observe any learning and memory deficiencies using the fear conditioning test (Figure 3.6 E,F). The lack of significant changes in the expression of presynaptic (synaptophysin) and postsynaptic (PSD-95) proteins in hippocampal lysates of TAM-injected Cx3cr1^{CreER} Dicer$^{fl/fl}$ and control mice provide some explanation for the lack of prominent behavior changes (Fig. 3.6 G-I). Thus, microglia dicer depletion does not result in broad reorganization of hippocampal circuits involved in learning and memory but rather results in specific perturbation of the stem cell pool. Future behavioral experiments focusing pattern-separation behavioral tasks, which are more strongly associated with adult neurogenesis in the dentate gyrus[83], will provide more useful insight on the functional consequences of altered stem cell numbers in hippocampi of Cx3cr1^{CreER} Dicer$^{fl/fl}$ mice. Notwithstanding, our study expands on the complexity of both adult microglia function and hippocampal stem cell niche, pointing to dicer dependent miRNAs as novel mechanistic regulators of cellular and tissue homeostasis in the brain.

Figure 3i

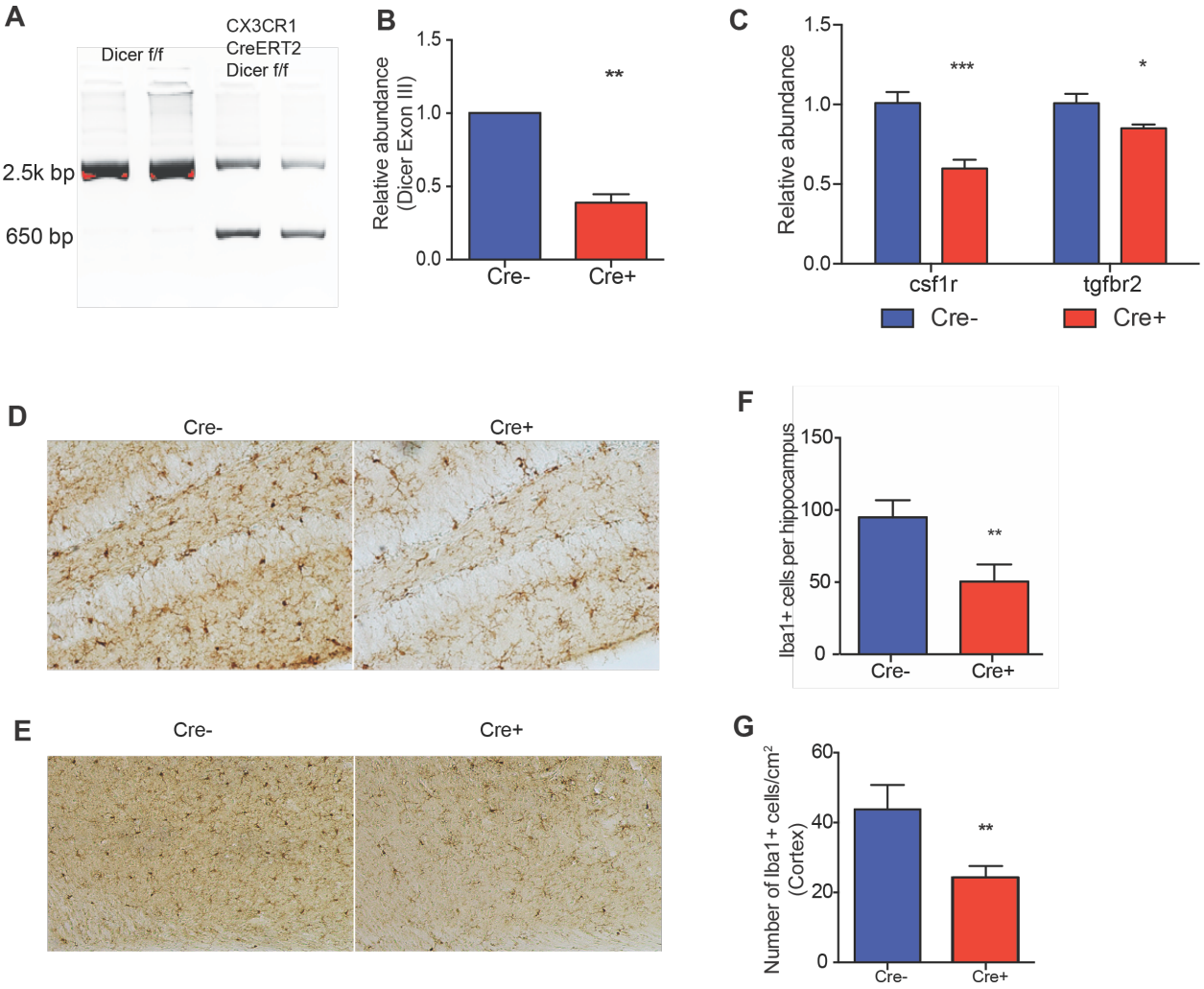

Figure 3.1. Deletion of *dicer* in adult microglia results in impairs microglia survival

(A) Genomic PCR of microglia acutely isolated from Dicer$^{fl/fl}$ (n=2) and Cx3cr1^{CreER} Dicer$^{fl/fl}$ (n=2) mice 8 weeks post TAM injection. (B) Quantitative real time PCR analysis of *dicer* exon III transcript levels in microglia acutely isolated from Dicer$^{fl/fl}$ (n=3) and Cx3cr1^{CreER} Dicer$^{fl/fl}$ (n=6) mice 8 weeks post TAM injection. (C) qRT PCR analysis of the expression of microglia survival genes, *Csf1r* and *Tgfbr2* in microglia acutely isolated from Dicer$^{fl/fl}$ (n=6) and Cx3cr1^{CreER} Dicer$^{fl/fl}$ (n=6) mice 8 weeks post TAM injection. Representative field of Iba1-postive microglia cells in the dentate gyrus (D) and cortex (E) of TAM-injected Dicer$^{fl/fl}$ (n=8) and Cx3cr1^{CreER} Dicer$^{fl/fl}$ (n=8) mice. Quantification of

microglia in the dentate gyrus (F) and cortex (G) of TAM-injected Dicer$^{fl/fl}$ and Cx3cr1^{CreER} Dicer$^{fl/fl}$ mice. Data represented as mean ± SEM; *P<0.05, **P<0.01, ***P<0.0001; t-test (B, C, F, G).

Figure 3ii

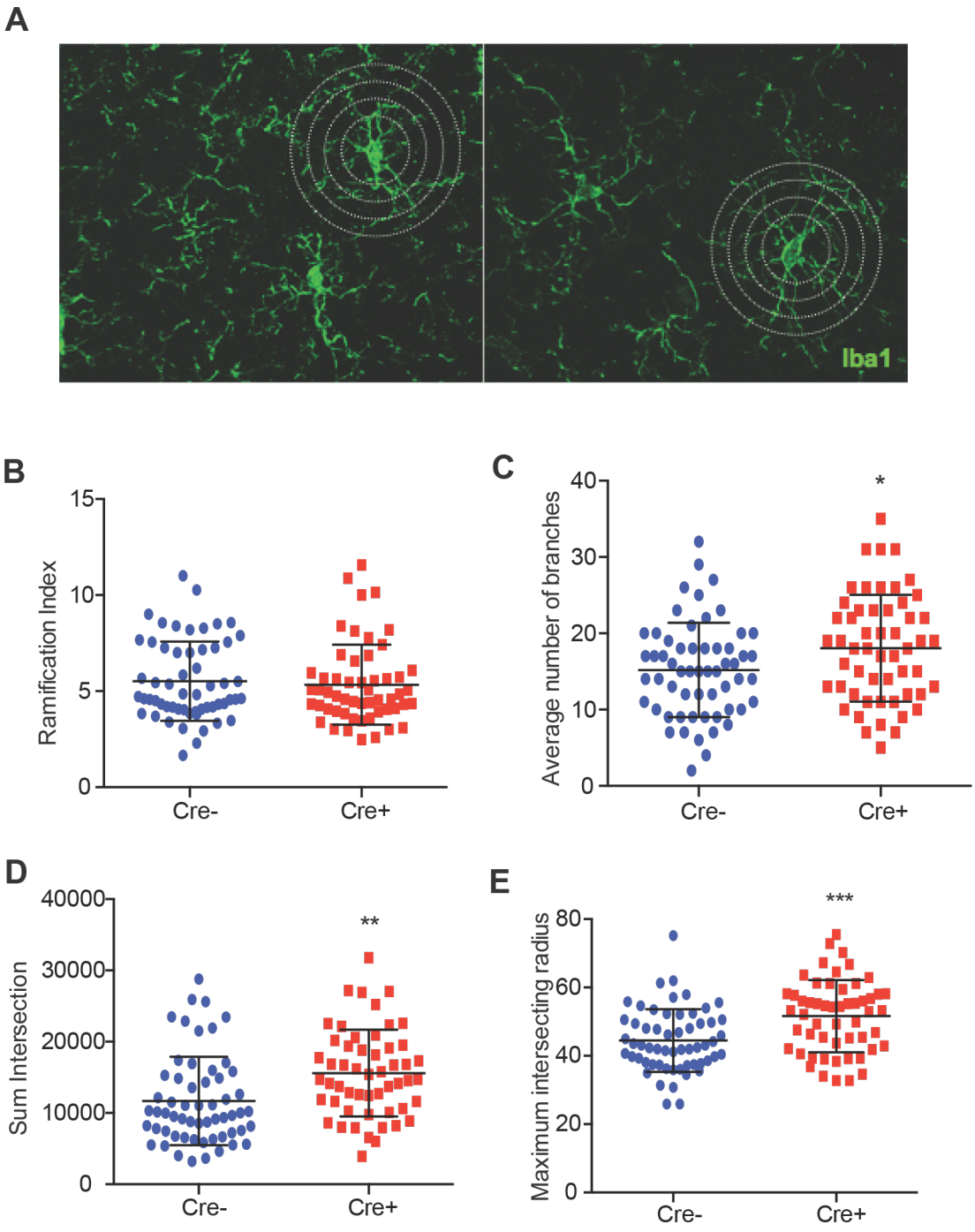

Figure 3.2. Characterization of morphological changes in dicer-depleted microglia

(A) Representative high magnification confocal images of tamoxifen injected Iba-1 positive microglia cells in Dicer$^{fl/fl}$ and Cx3cr1^{CreER} Dicer$^{fl/fl}$ brains. (B-E) Sholl analyses of

microglia morphology in Dicer$^{fl/fl}$ and Cx3cr1^{CreER} Dicer$^{fl/fl}$ brains, showing ramification, index, average number of branches, sum of intersections and maximum intersection radius. Data represented as mean ± SEM; *P<0.05, **P<0.01, ***P<0.0001; t-test (B-E). n = 4 per group for Dicer$^{fl/fl}$ and Cx3cr1^{CreER} Dicer$^{fl/fl}$ mice.

Figure 3iii

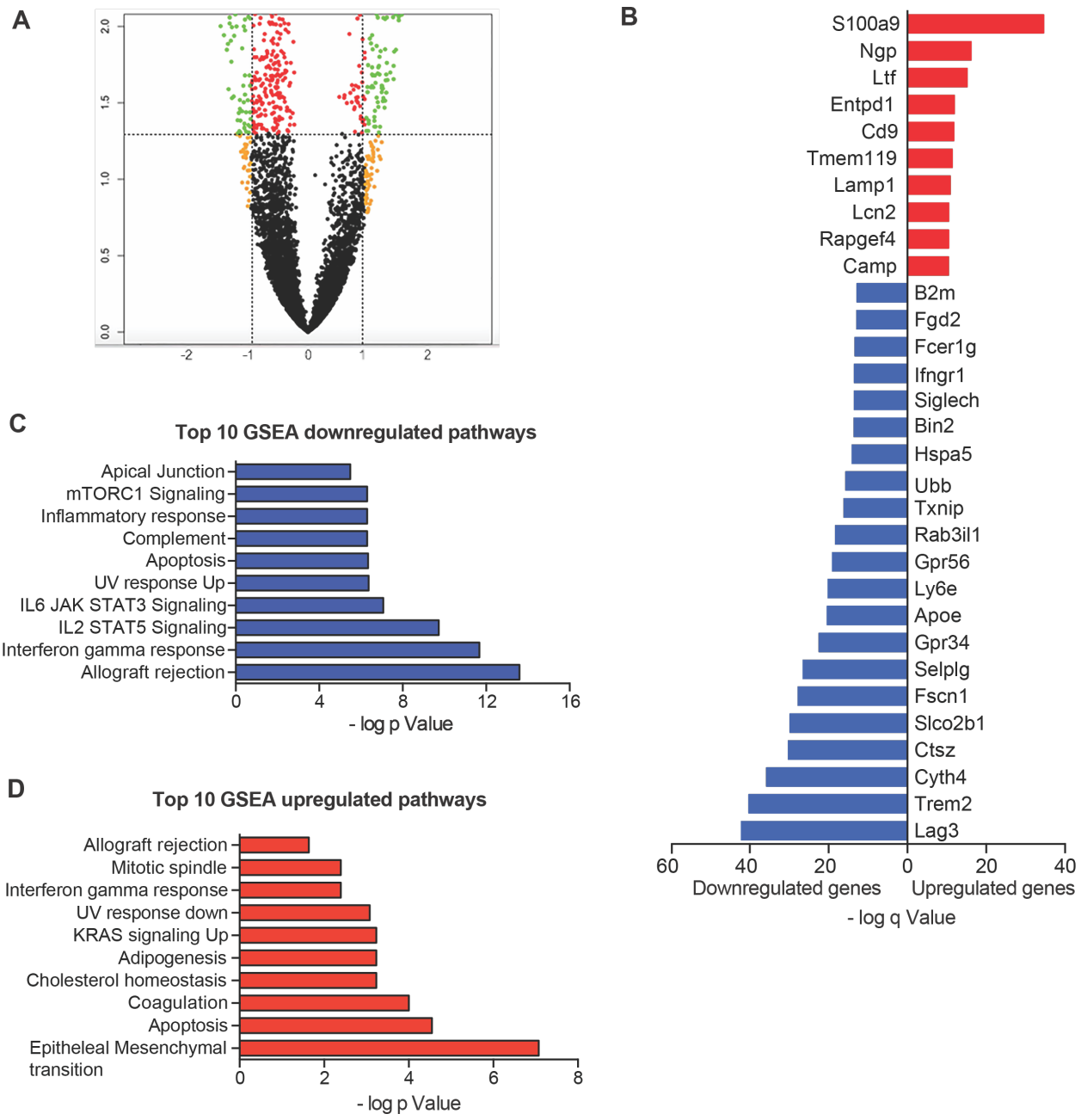

Figure 3.3. Transcriptional analyses of dicer depleted microglia highlighting significant changes in apoptotic and inflammatory genes

(A) Volcano plot showing z scores derived from average molecule counts of genes in acutely isolated Dicer$^{fl/fl}$ and Cx3cr1^{CreER} Dicer$^{fl/fl}$ microglia 8 weeks post TAM injection, as determined by high throughput RNA sequencing ((yellow = 2 fold change, red = $p < 0.05$,

green = 2 fold change and $p < 0.05$). (B) Top upregulated and downregulated differentially expressed genes in Cx3cr1^{CreER} Dicer$^{fl/fl}$ and Dicer$^{fl/fl}$ microglia. Gene set enrichment analysis showing pathways enriched in downregulated (C) and upregulated (D) differentially expressed genes in TAM injected in Cx3cr1^{CreER} Dicer$^{fl/fl}$ microglia.

Figure 3iv

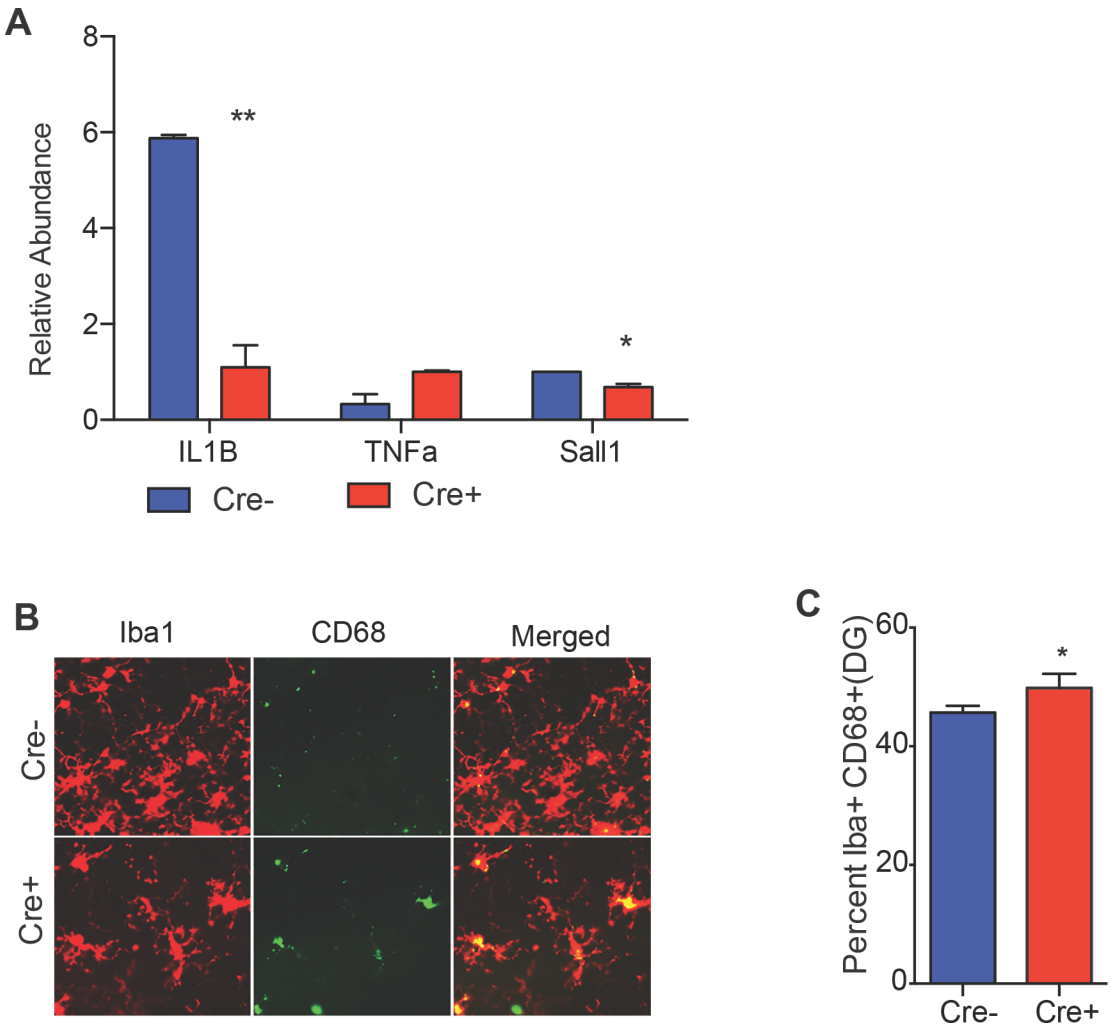

Figure 3.4. Validation of inflammatory activation of dicer-depleted microglia

(A) qRT PCR analysis of inflammatory genes, *IL1β* and *TNFα,* and microglia identity gene, *Sall1*, TAM injected Cx3cr1^{CreER} Dicer$^{fl/fl}$ and Dicer$^{fl/fl}$ microglia. (B) Representative images of TAM injected Cx3cr1^{CreER} Dicer$^{fl/fl}$ and Dicer$^{fl/fl}$ brains fluorescently labeled with microglia marker, Iba1, and activation marker, CD68. (C) Quantification of Iba1 microglia positive for activation marker, CD68, in the dentate gyrus of injected Cx3cr1^{CreER} Dicer$^{fl/fl}$ and Dicer$^{fl/fl}$ brains. Data represented as mean ± SEM; **P*<0.05, ***P*<0.01; t-test (B,C).

Figure 3v

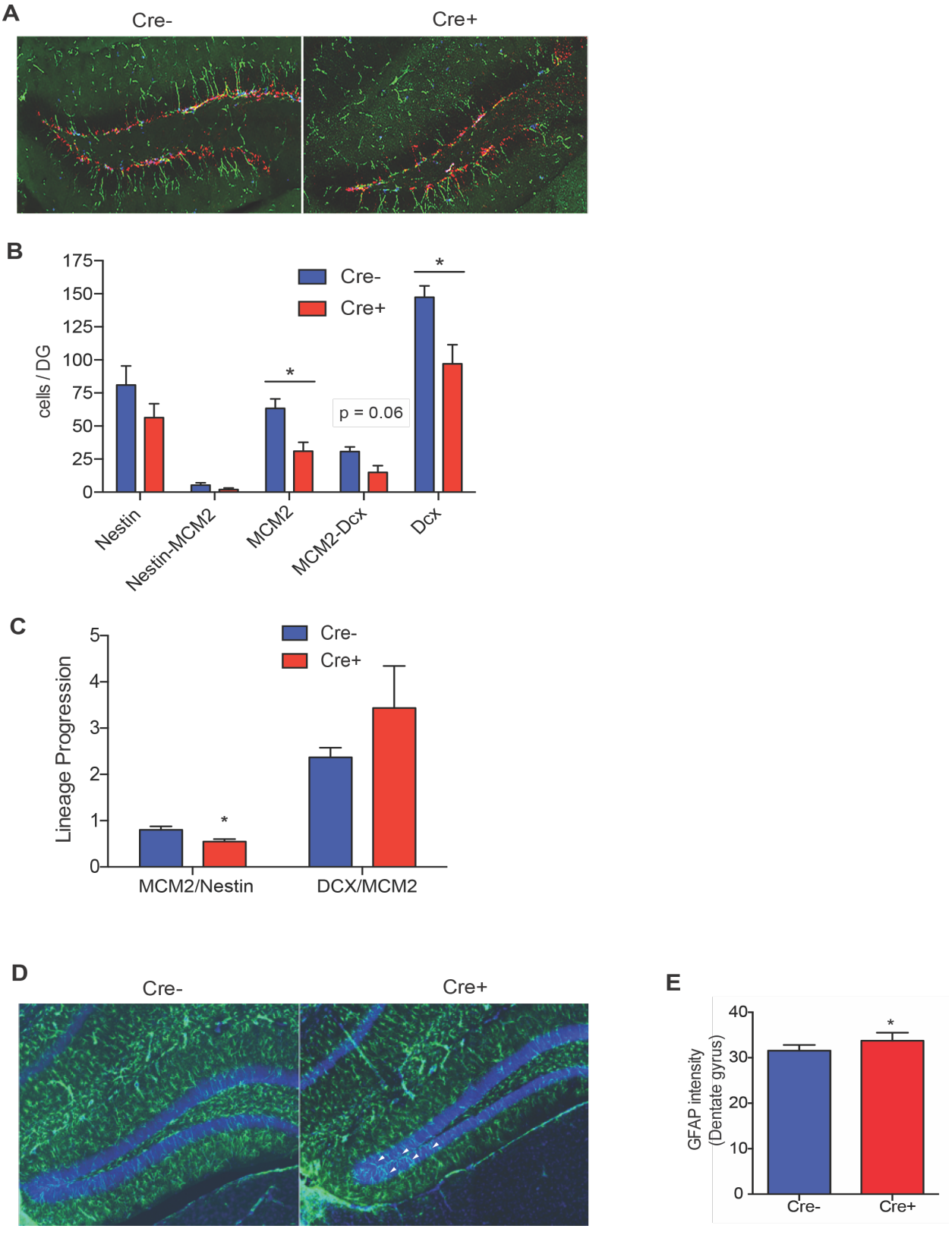
A
Cre-
Cre+
B
cells / DG
175
150
125
100
75
50
25
0
Cre-
Cre+
*
*
p = 0.06
Nestin
Nestin-MCM2
MCM2
MCM2-Dcx
Dcx
C
Lineage Progression
5
4
3
2
1
0
Cre-
Cre+
*
MCM2/Nestin
DCX/MCM2
D
Cre-
Cre+
E
GFAP intensity
(Dentate gyrus)
40
30
20
10
0
*
Cre-
Cre+

Figure 3.5. Microglia dicer depletion alters the cellular composition of the hippocampal stem cell niche

(A) Representative images of TAM injected Cx3cr1^{CreER} Dicer$^{fl/fl}$ and Dicer$^{fl/fl}$ dentate gyrus fluorescently labeled with Nestin (green), MCM (blue) and doublecortin (red). (B) Quantification of Nestin-, MCM- and doublecortin positive cells in the DG of TAM injected Cx3cr1^{CreER} Dicer$^{fl/fl}$ and Dicer$^{fl/fl}$ mice (n = 4 per group). (C) Lineage progression analysis of hippocampal stem cells in TAM injected Cx3cr1^{CreER} Dicer$^{fl/fl}$ and Dicer$^{fl/fl}$ mice. (D) Immunofluorescent labeling of GFAP in the DG of TAM injected Cx3cr1^{CreER} Dicer$^{fl/fl}$ and Dicer$^{fl/fl}$ mice. (F) Quantification of GFAP intensity in the granule cell layer of TAM injected Cx3cr1^{CreER} Dicer$^{fl/fl}$ and Dicer$^{fl/fl}$ mice. Data represented as mean ± SEM; *P<0.05, t-test (B-D).

Figure 3vi

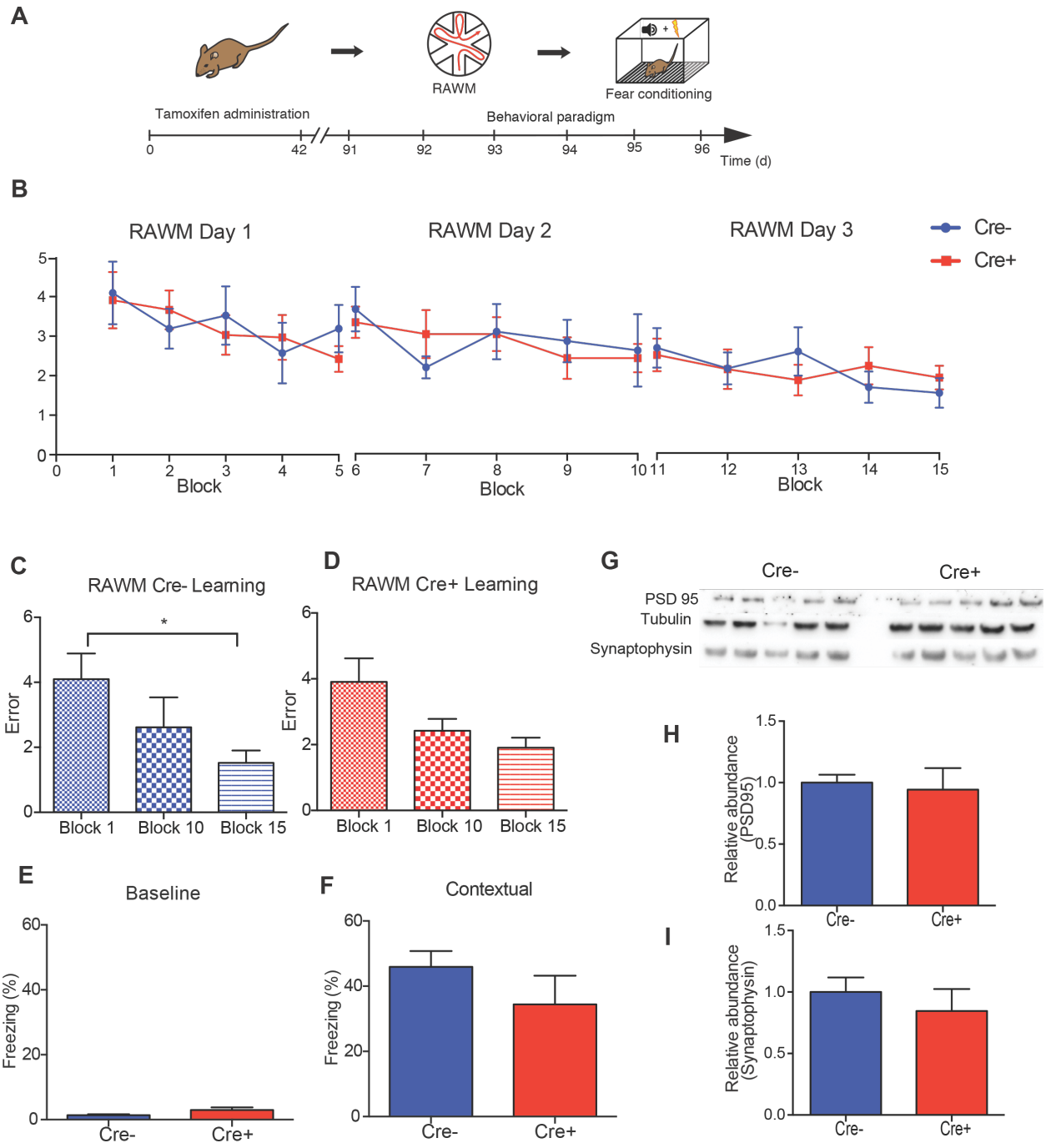

Figure 3.6 Dicer depletion in adult microglia does not result in significant changes in hippocampal-dependent behavior and synapse number.

(A) Schematic illustrating chronological order used for TAM injection and cognitive testing in Cx3cr1^{CreER} Dicer$^{fl/fl}$ and Dicer$^{fl/fl}$ mice. (B) Hippocampal learning and memory was

accessed by RAWM (B) and contextual fear conditioning (F). (B) Number of entry arm errors prior to finding escape platform. Analysis of learning in TAM injected Dicer$^{fl/fl}$ (C) and Cx3cr1^{CreER} Dicer$^{fl/fl}$ (D) mice. (E,F) Contextual fear conditioning results showing percent freezing at baseline and during testing of contextual memory during fear conditioning behavioral assay of TAM injected Cx3cr1^{CreER} Dicer$^{fl/fl}$ and Dicer$^{fl/fl}$ mice. (G) Representative Western blot probes of synaptic proteins (synaptophysin and PSD 95) in TAM-injected Cx3cr1^{CreER} Dicer$^{fl/fl}$ and Dicer$^{fl/fl}$ mice hippocampal lysates. (H,I) Quantification of Western blot intensities of synaptic proteins in TAM-injected Cx3cr1^{CreER} Dicer$^{fl/fl}$ and Dicer$^{fl/fl}$ mice hippocampal lysates. Data represented as mean ± SEM; *P<0.05, repeated measures ANOVA, Bonferroni post-hoc test (B, C, D) (n = 8 per group), t-test (H,I, n = 5 per group).

CHAPTER 4:

MATERIALS AND METHODS

4.1 Animal studies

4.1.i Animal Models. The following mouse lines were used: C57BL/6 (The Jackson Laboratory), C57BL/6 aged mice (National Institutes of Aging), C3H/HeSnJ wildtype and ashen mutant mice (The Jackson Laboratory). Cx3cr1^{CreER} Dicer$^{fl/fl}$ mice were generated by first crossing Cx3cr1^{CreER} mice with Dicer$^{fl/fl}$ mice, and then crossing the resultant F1 progeny to produce mice homozygous for the floxed allele. All studies were done in male mice. The numbers of mice used to result in statistically significant differences was calculated using standard power calculations with $\alpha = 0.05$ and a power of 0.8. Power and size were calculated based on with the respective tests, variability of the assays and inter-individual differences within groups using http://www.stat.uiowa.edu/~rlenth/Power/index.html. Mice were housed under specific pathogen-free conditions under a 12 h light-dark cycle and all animal handling and use was in accordance with institutional guidelines approved by the University of California San Francisco IACUC.

4.1.ii Behavioral paradigms

4.1.ii.a Contextual fear conditioning. Our paradigm followed previously published techniques[84]. Mice learned to associate the environmental context (fear-conditioning chamber) with an aversive stimulus (mild foot shock; unconditioned stimulus, US), which enabled testing for hippocampal-dependent contextual fear conditioning. The mild foot shock was paired with a light and tone cue (conditioned stimulus, CS) in order to also assess amygdala-dependent cued fear conditioning. Conditioned fear was displayed as freezing behavior. Specific training parameters were as follows: tone duration, 30 s; level, 70 dB, 2 kHz; shock duration, 2 s; intensity, 0.6 mA. On day 1, each mouse was placed

in a fear-conditioning chamber and allowed to explore for 2 min before delivery of a 30-s tone (70 dB) ending with a 2-s foot shock (0.6 mA). Two minutes later, a second CS-US pair was delivered. On day 2, each mouse was first placed in the fear-conditioning chamber containing the same exact context but with no administration of a CS or foot shock. Freezing was analyzed for 1–3 min. One hour later, the mice were placed in a new context containing a different odor, cleaning solution, floor texture, chamber walls and shape. Animals were allowed to explore for 2 min before being re-exposed to the CS. Freezing was analyzed for 1–3 min. Freezing was measured using a FreezeScan video tracking system and software (Cleversys, Inc).

4.1.ii.b Radial Arm Water Maze (RAWM). Our RAWM paradigm followed a previously described protocol[85]. The goal arm location containing a platform remained constant throughout the training and testing phases, and the start arm was changed during each trial. On day 1 during the training phase, mice were trained for 15 trials, with trials alternating between a visible and a hidden platform. On day 2 during the testing phase, mice were tested for 15 trials with a hidden platform. Entry into an incorrect arm was scored as an error, and errors were averaged over the training blocks (three consecutive trials).

4.1.iii Tamoxifen administration. For induction of Cre recombinase, 6- to 8-week old Cx3cr1^{CreER} mice were subcutaneously injected with 4 mg tamoxifen (TAM, Sigma) dissolved in 200 µl of sunflower oil and ethanol (90:10, v/v) at two time points 48 hours apart. Behavioral analyses were performed on injected animals 6 weeks post injection, when applicable, and mice were sacrificed and tissue harvested at 8 weeks post injection.

4.1.iv Stereotaxic injections. Animals were placed in a stereotaxic frame and anesthetized with 2% isoflurane (2L/min oxygen flow rate) delivered through an anesthesia nose cone. Ophthalmic eye ointment (Puralube Vet Ointment, Dechra) was applied to the cornea to prevent desiccation during surgery. The area around the incision was trimmed. Solutions (GW4869 or DMSO dissolved in PBS) were injected unilaterally into the DG of the dorsal hippocampi using the following coordinates: (from bregma) anterior = -2mm, lateral = 1.5mm, (from skull surface) height = -2.1mm. A 2.5 µl volume was injected stereotaxically over 10 minutes (injection speed: 0.20µl/min) using a 5 µl 26s gauge Hamilton syringe. To limit reflux along the injection track, the needle was maintained *in situ* for four minutes, slowly pulled out half way and kept in position for an additional two minutes. The skin was closed using silk suture. Each mouse was injected subcutaneously with the analgesic Buprenex. Mice were single-housed and monitored during recovery. Mice were perfused 7 days post-injection for tissue analyses.

4.1.v Intracerebroventricular (ICV) delivery

Osmotic pumps were first attached to an L-shaped cannula via a 3.5 cm tubing according to manufacturer's instructions (Model 1002, Brain infusion kit 3). The assembly was preincubated in normal saline at 37C for 48-72hrs to activate pump prior to surgical implantation. The assembly was surgically implanted into the left ventricle of each mouse using a stereotactic apparatus, using the following coordinates: (from bregma) anterior = -0.4mm, lateral = 1.0mm, (from skull surface) height = -2.5mm. The osmotic pumps were place under the skin of the left flank by making a subcutaneous pocket with a curved, blunt scissors. Cannula were secured by gluing to the skull surface, prior to stitching the skin back together. Pumps contained either 10ng/ml IFNγ dissolved in PBS or just PBS.

Pumps were loaded with a maximum volume of 100μl and pumped at a rate of 6μl per day. Pumps were implanted for either 3 or 7 days, before mice were sacrificed and brains harvested for histology, RNA and protein analyses.

5.2 Microglia culture and isolation

4.2.i BV2 microglia culture. The BV2 microglia cell line[86] was maintained in growth media – DMEM (Thermo Fisher) supplemented with 10% heat-inactivated fetal bovine serum (FBS, Hyclone) and 1% penicillin/streptomycin (Life Technologies) in HERAcell 150i incubators (Caisson Labs) at 37C with 5% CO2. BV2 microglia were serially passaged once plates reached 80-90% confluency.

4.2.ii Isolation and culture of postnatal primary microglia*:* Primary microglial cells were harvested from mouse pups at postnatal day 3–6 (P3–P6). Briefly, the brain cortices were isolated and minced. Tissues were dissociated in 0.25% Trypsin-EDTA for 20 min at 37°C and agitated every 5 min. Trypsin was neutralized with complete medium (DMEM (Thermo Fisher) supplemented with 10% heat-inactivated fetal bovine serum (FBS, Hyclone)), and were filtered through 70μm cell strainers (BD Falcon) and pelleted by centrifugation at 1500 rpm. Mixed glial cultures were maintained in growth medium at 37°C and 5% CO2 for 7–10 d *in vitro*. Once bright round cells began to appear in the mixed glial cultures, recombinant mouse granulocyte macrophage colony stimulating factor (1ng/ml, Life Technologies) was added to promote microglia proliferation. Primary microglial cells were harvested by mechanical agitation after 48-72 hours and plated on poly-L lysine coated t-75 flasks (Corning) in growth media and used for functional assays within 72 hours of purification. Functional assays were performed in serum free media.

4.2.iii Isolation of adult primary mouse microglia. Wild type mice (3 and 24 months, National Institutes of Aging) and 3.5-4 month old tamoxifen injected Cx3cr1^{CreER} Dicer$^{fl/fl}$ or Dicer$^{fl/fl}$ mice were transcardially perfused with PBS, brains were gently minced, and dissociated into single cells using the Neural Tissue Dissociation Kit P (Miltenyl Biotec). Cells were washed with Hank's Balanced Salt Solution and resuspended in PBS containing 0.5% FBS and 2mM EDTA (MACS buffer). Myelin removal was performed by incubation of the cell suspension with a ferric anti-myelin antibody and passed through a LS separation column placed in a magnetic holder (Miltenyl Biotec). Microglia enrichment was performed on the flow through cells by incubation with CD11b microbeads (Miltenyl Biotec), washed with MACS buffer and applied to a LS separation column placed in a magnetic holder (Miltenyl Biotec). The columns were removed from the magnetic field and labeled cells were flushed from the column with MACS buffer. Flow cytometry on the labeled cells confirmed ~95% microglia purity. Isolated microglia were immediately processed for RNA isolation without culture or frozen in RNA stabilization buffer and frozen (RNAlater-ICE, Ambion). Microglia isolated from tamoxifen injected Cx3cr1^{CreER} Dicer$^{fl/fl}$ or Dicer$^{fl/fl}$ mice and RNA sequencing libraries were prepared. All samples were analyzed by quantitative PCR to assess expression of inflammatory (*IL1β*, *TNFα*, *IL4*), microglia survival/identity (*Tgfbr2*, *Csf1r*, *Sall1*) and exosome regulatory (*rab27a*) genes. *IL1β*, *TNFα*, and *IL4* expression was assessed using Taqman primers (Life Technologies). Sequences of other primers used: *Csf1r* (CGCCGAAGTGGGATTCAA; CAG CGTTGAGACTGAGAGCC), *Sall1* (CCCGTGAGCGGCTGATGTTTGAG; TGGGGCGACTTGGTTGAC CCT), and *Tgfbr2* (AACGACTTGACCTGTTGCCTGT; CTTCCGGGGCCATGTATCTT).

4.3 Exosome isolation

4.3.i Isolation from microglia culture media: BV2 or primary microglia were grown to ~60-70% confluency, thoroughly washed with PBS, and incubated in macrophage serum free media (MSFM) with or without interferon gamma. MSFM was collected after overnight incubation and processed for exosome isolation by differential ultracentrifugation, as previously described[59]. Briefly, media was spun for 300 x *g* for 10 min to pellet live cells. Dead cells and apoptotic bodies were removed by sequential spins of 2,000 x *g* and 10,000 x *g*, respectively. The supernatant was then passed through a 0.22μm syringe filter unit. Exosomes were pelleted finally pelleted by centrifuging at 100,000 x *g* for 90 mins. Pelleted exosomes were then washed with 30ml filtered PBS at 100,000 x *g* for 90 mins. Ultracentrifugation was done using SW 28 or Ti 70.1 rotors on a Beckmann Coulter Optima XPN-80 ultracentrifugation. For mass spectrometry and Taqman microRNA profiling, exosomes were further concentrated using total exosome isolation buffer (Life Technologies).

4.3.ii Isolation of interstitial brain exosomes: Mouse brains were processed for exosome isolation following published techniques[37]. Briefly, freshly perfused or frozen hemibrains were gently homogenized in dissociation buffer - Hibernate E (BrainBits Inc.) plus papain (Wormingthon) and incubated at 37C for 15 mins. Digestion was quenched by diluting in twice the volume of Hibernate E, filtered through a 40μm mesh to eliminate debris. Further filtration was performed using a 0.22μm syringe filter. Differential ultracentrifugation was performed as described above to isolate exosomes. To concentrate exosomes into a smaller volume, the resuspended pellet from differential ultracentrifugation was incubated with total exosome isolation buffer (Life Technologies)

overnight. Samples were centrifuged at 10000 x *g* for 60 mins, resuspended in sterile PBS, and utilized for downstream applications or stored at -80C.

4.4 Exosome characterization.

4.4.i Nanoparticle tracking: Size distribution of the purified exosomes was determined using nanoparticle tracking analysis (Malvern Inc.). To get consistent measurements on the nanoparticle tracking software, purified exosomes were diluted hundred fold or more in cold, filtered PBS to obtain an ideal vesicle concentration range. 3-4 measurements of each sample were collected and concentration values were averaged.

4.4.ii Transmission electron microscopy: Exosomes were fixed in EM grade formaldehyde immediately following isolation. Negative staining was performed on a small aliquot of the fixed exosomes, which were loaded on Formvar-carbon coated EM grids and negative staining was performed as previously described[59]. Scanning electron microscopy allowed visualization of vesicle structure and size.

4.4.iii Western Blot: Exosomes were lysed in RIPA buffer (500 mM Tris, pH 7.4, 150 mM NaCl, 0.5% sodium deoxycholate, 1% NP40, 0.1% SDS, and complete protease inhibitors; Roche) or exosome lysis buffer (Life Technologies). Lysates were stored at -80C or used immediately for protein analysis. Lysates were mixed with 4x NuPage LDS loading buffer (Invitrogen) and loaded on a 10% SDS polyacrylamide gradient gel (Invitrogen) and subsequently transferred onto a nitrocellulose membrane. The blots were blocked in 5% milk in Tris-Buffered Saline with Tween (TBST) and incubated with rat anti-CD63 (1:500; MBL; clone: R5G2), rat anti-CD9 (1:2000, Biosciences; clone: KMC8), and rat anti-LAMP2 (1:200, Santa Cruz; clone: M3/84). CD9 and CD63 were run in non-reduced conditions. Protein lysates from BV2 microglia were probed with rabbit

anti-phospho p65 (Ser 536, Cell Signaling), rabbit anti-phospho Stat1 (Tyr701, Cell Signaling), mouse anti-tubulin (Proteintech), and mouse anti-Gapdh (Sigma). Horseradish peroxidase-conjugated secondary antibodies (1:5000, GE Healthcare; NA934) and an ECL kit (Biorad) were used to detect protein signals. Multiple exposures were taken to select images with appropriate exposure (Biorad Imager). Selected images were exported at 300dpi and quantified using ImageJ software (Version 1.46k). Exosome Western blots were normalized to total protein concentration.

4.4.iv Mass Spectrometry

Peptide Digestion: Pooled exosomes were lysed and denatured in an aqueous solution of 50mM TEAB and 0.1% SDS (Sigma), Protein concentration was measured using a BCA assay, and 25-50μg of each sample placed in a speedvac at 60C. Samples were reduced in 500mM TECP for 1 hour at 60C and alkylated by addition of 10mM iodoacetamide for 15 mins at room temperature. Trypsin (spectrometry grade, Promega) was added to the solution at ratio of 1:25 and incubate overnight at 37C. Detergent removal was performed on the samples following manufacturer's instructions (Thermo Fisher). Samples placed in a speedvac until nearly dry and resuspended in to a concentration of 1 μg/μl in LCMS buffer A and stored at -80C.

Liquid chromatography mass spectrometry (LCMS):

Peptides were separated using a nanoLC Ultra 2D Plus cHIPLC system (SCIEX) in serial two column mode with two nano cHIPLC columns (75 μm x 15 cm ChromXP C18-CL 3 μm 300 Å). The peptides were initially loaded onto the first column and washed with buffer A (2% acetonitrile/98% H_2O/0.1% formic acid) for 30 min at a flow rate of 0.5 μL/min. The elution gradient was 2-30% buffer B (98% acetonitrile/2% H_2O/0.1% formic acid) over 120

min at 300 nL/min. The TripleTOF 5600 equipped with a NanoSpray III source (SCIEX) was used for MS data acquisition. The IDA method was constructed to acquire a TOF MS survey scan at >30,000 resolution for 0.25 msec, followed by 20 MS/MS spectra in 3 s at >15,000 resolution with an exclusion time of 15 s. Protein identification was performed by using ProteinPilot v5.0 software (SCIEX) and the UniProt SwissProt v2011605 Mus musculus database using integrated false discovery rate analysis function with a concatenated reversed database. Data were searched in Thorough mode with tryspin digestion and iodoacetamide modification.

Alignment:

Proteins detected with local false discovery rate (FDR) ≤5% from each individual experiment were aligned to a search result from all samples searched together (Master) to create a comprehensive list of proteins and compare groups. The Master list for alignment included191 proteins detected with a global FDR ≤1%.

4.4.v microRNA profiling. Exosomes were pooled from several experiments to have sufficient input material. Pooled samples of BV2 microglia exosomes lysed and processed for microRNA isolation using the miRNeasy kit according to manufacturer's instructions (Qiagen). To measure miRNA composition, reverse transcription and preamplification was performed using Rodent miRNA primer pool A and B on 300ng of input RNA isolated from pooled activated and unactivated BV2 exosomes (Life Technologies). To measure the abundance of individual miRNA species, samples were loaded into Taqman Rodent Array microRNA A and B cards (version 3.0, Applied Biosystems) and quantitative PCR was performed. Resultant Ct values for each sample were normalized to U6 levels, and fold change was determined relative to untreated exosome miRNAs.

4.5 Exosome functional assays

4.5.i Exosome uptake assay

Purified exosomes were fluorescently labeled using lipophilic dye, PKH-67, according to the manufacturer's instructions (Sigma). Briefly, purified exosomes were incubated with PKH-6 for 3 mins, and then treated with PBS-BSA solution to quench excess dye. Labeled exosomes were washed subsequently washed with cold PBS and pelleted before proceeding with assays. Recipient microglia were plated in 24 well dishes at a density of 10000 cells per well and were incubated with labeled exosomes or vehicle overnight at 37C. Uptake was determined by measuring green fluorescent signal in recipient microglia via flow cytometry (Accuri B6, Biosciences). To confirm internalization, uptake assay was repeated in the presence of actin polymerization inhibitor, catecholamine D (Sigma) or clathrin endocytosis inhibitor, pipstop 2 (Fisher). Cells were pretreated with inhibitors for 30 mins before introduction of labeled exosomes. Uptake assay was performed for 3 hours to minimize potential toxic effects of inhibitors. After 3 hours, cells were thoroughly washed and analyzed by flow cytometry as above.

4.5.ii Flow Cytometry. All flow cytometry experiments were performed on an Accuri C6 machine (BD Biosciences). Cells were resuspended in FACS buffer (sterile PBS plus 1.5% FBS) and maintained on ice until analysis. In all experiments, appropriate negative controls were used to establish correct gaiting parameters. For phagocytosis assays, events analyzed were gated to exclude the visualization of non-internalized latex beads. Samples were analyzed automatically using the Accuri C6 software and subsequent statistical analysis done on GraphPad Software.

4.5.iii Live cell microscopy.

BV2 microglia were plated at a density of 1000-2000 cells per well primaria 24 well plates (Fischer) coverslips. Cells were allowed to rest overnight and then stimulated with freshly isolated and PKH-67 fluorescently labeled exosomes. Cells were allowed to equilibrate with exosomes for 3 hours before proceeding with live imaging. Live imaging was performed on a Leica chamber system (). Briefly, the chamber was warmed to 37C and filled with 5% CO2 prior to introduction of cells. Representative areas for were clearly defined for repeated imaging – 2 regions per well, 3 wells per group. Images were collected every 30 mins, for 16 hours for vehicle and exosome treated microglia. Individual images were exported as TIF files, and analyzed using Fiji Software. Round cells were defined as cells with no process extending from cell body, whereas ramified cells contained 3 or more processes extending from cell body. Cell morphology was compared between the third and third from last images taken to determine exosome effect.

4.5.iv Direct exosome stimulation assays. Exosomes isolated from IFNγ-treated microglia were utilized for direct stimulation assays immediately after isolation. Exosomes were added to recipient microglia plated at density of 30000 cells per well. Exosomes isolated from different number of producing cells were utilized for the stimulation assays to determine a dose response range in recipient microglia. Data presented are from stimulation assays performed at 10:1, 20:1 and 30:1 ratios of producing to recipient cells. Cells were analyzed for functional changes in phagocytosis using latex bead assay, and inflammation was assessed by quantitative PCR and Western blot of immune related genes.

4.5.iv.a Latex bead phagocytosis Assay. BV2 or primary microglia were plated in 24-well plates directly or on poly-L lysine coated coverslips at density of 8,000 to 15,000 cells per well and maintained in DMEM with 10% FBS, with antibiotics for 1-2 days. Media was then replaced with macrophage serum free media (MSFM) and cells were allowed to equilibrate overnight. To perform phagocytosis assay, latex beads (5μm, internally dyed with the fluorophore Flash Red; Bangs Laboratories) were first opsonized by incubation with 50:50 solution of FBS and PBS at 37C for 30mins. Following opsonization, cells were treated with beads at a concentration of ten beads per cell for 30 – 60 min at 37C. Isolecthin was added to the samples in the last 5 minutes to label cells. Media was removed and microglia were thoroughly washed with cold PBS to stop bead internalization and eliminate cell free beads. Cells plated on coverslips were then fixed with 3% paraformaldehyde, imaged using a Zeiss epifluorescence microscope and counted on the ImageJ software. Alternatively, cells directly plated in 24 wells were trypsizinized, washed and analyzed using the Accuri C6 machine. Gating strategy used excluded free beads from analysis.

4.5.iv.b RNA sequencing library preparation and analysis.

RNA sequencing libraries were prepared using freshly isolated RNA from vehicle and exosome-treated primary microglia using a previously published protocol[87]. Briefly, Poly-A RNA was collected from samples and then reverse transcribed using template switching primers (Nextera XT DNA sample preparation kit, Illumina). Resultant cDNA was then preamplified using high fidelity PCR (Kapa Biosystems and purified using Ampure XP DNA SPRI Beads (Beckman-Coulter). Quantitative PCR was performed to confirm the presence microglia enriched genes. Subsequently, samples were tagmented, indexed

with barcodes and amplified to produce sequence quality libraries (Nextera XT Index Kit, Illumina). RNA sequencing was performed using the Illumina Next Generation Platform and sequencing results were analyzed using the online the Illumina BaseSpace platform. Paired sequence reads were first concatenated and then passed through the BaseSpace RNA express program, which performed STAR and mouse genome alignment of reads, gene clustering, and differential expression analysis (q value < 0.05). Differentially expressed genes were exported for further analysis and visualization on R software. Ontology analysis was performed on the list of differentially expressed genes using Panther Biology system. qPCR was performed to validate gene targets found to be differentially expressed in exosome- compared to vehicle-treated microglia. Primers used for qPCR are:

Sod2 (GCGCTGGCCAAGGGAGATGTT; ATGGCCCCCGCCATTGAACTT)

Ccl5 (CACCATATGGCTCGGACACC; GTGACAAACACGACTGCAAG)

C3 (CCAGCTCCCCATTAGCTCTG; GCACTTGCCTCTTTAGGAAGTC)

Gbp2 (CAGCTGCACTATGTGACGGA; CAGTCGCGGCTCATTAAAGC)

Gapdh (

4.6 Quantitative real time PCR analysis of microglia inflammation.

4.6.i RNA expression: Microglia were treated with interferon gamma (IFNγ, Life Technologies), lipopolysaccharide (LPS, Sigma), or polyribocytidilic acid (poly I:C, Sigma) at 1-10ng/ml concentration for 6 or 24 hours. RNA was isolation from cells using standard Trizol-chloform phase separation and ethanol precipitation. RNA concentration and quality were measure on the Citation 5 Image reader (Biotek). Sample RNA was reversed transcribed and cDNA analyzed by qPCR to measure relative expression levels of various

inflammatory molecules. *IL1β, TNFα*, *Stat1* and *myd88* were analyzed using Taqman primers (Life Technologies) on a CFX384 Real Time System (BioRad).

4.6.ii microRNA expression: Total RNA isolated from interferon gamma (IFNγ, Life Technologies) treated microglia were reverse transcribed using taqman miRNA assays (Life Technologies, mmu-miR-155, has-miR-125-5p, has-miR-103, snU6). Following reverse transcription, real time PCR was performed to measure expression of miRNAs across different samples. Expression was normalized to U6 as a housekeeping miRNA.

4.7 Immunohistochemistry. Tissue processing and immunohistochemistry was performed on free-floating sections following standard published techniques[88]. Briefly, mice were anesthetized with 400 mg/kg avertin (Sigma-Aldrich) and transcardially perfused with 0.9% saline. Brains were removed and fixed in phosphate-buffered 4% paraformaldehyde, pH 7.4, at 4°C for 48 h before they were sunk through 30% sucrose for cryoprotection. Brains were then sectioned coronally at 40 μm with a cryomicrotome (Zeiss, Inc.) and stored in cryoprotective medium. Primary antibodies were: rabbit anti-Iba1 (1:2000; Dako), rat anti-CD68 (1:200, Millipore), rat anti-CD63 (1:100; Santa Cruz; clone: M13), rat anti-LAMP2 (1:200, Santa Cruz; clone: M3/84). After overnight incubation, primary antibody staining was revealed using fluorescence conjugated secondary antibodies (Life Technologies).

4.8 Viral Infection. BV2 microglia were maintained in DMEM media containing 10% FBS. Cells were transduced with lentivirus (LV) containing an shRNA plasmid targeting mouse rab27a or a scramble shRNA sequence using a previously published transduction protocol[89]. The lentivirus also expressed a copped GFP, to allow visualization of infected cells. BV2 were plated at a density of 1000 cells per well in 96-well plates, and infected

at a multiplicity of infection of 50 or 100 in the presence of polybrene (8 mg/ml). After overnight infection, media was removed and replaced with normal growth media. Cells were allowed to grow for an additional 72 hours, split into 24 well dishes and treated with puromycin to select for infected cells. Selection was performed for 48 hours and surviving cells were assessed for GFP expression using the Accuri C6 machine. Knockdown was confirmed qPCR assessment of rab27a transcript levels, due to lack of a good commercial antibody. LV plasmids were prepared by performing lipofectamine transfection of 293T cells with vectors expressing desired transgene, Pax2, and VSVG. Following overnight incubation, transfection media was replaced with viral production media, DMEM plus viral boost reagent (Alstem). Virus production media was collected the following day and processed for virus isolation. Cells and cellular debris were pelleted and media was filtered through a 0.45 mesh (Maine Productions).

4.9 Data and statistical analyses. All experiments were randomized and blinded by an independent researcher prior to pharmacological treatment or assessment of genetic mouse models. Researchers remained blinded throughout histological, biochemical and behavioral assessments. Groups were un-blinded at the end of each experiment upon statistical analysis. Data are expressed as mean ± SEM. The distribution of data in each set of experiments was tested for normality using D'Agostino-Pearson omnibus test or Shapiro-Wilk test. No significant differences in variance between groups were detected using an F test. Statistical analysis was performed with Prism 5.0 software (GraphPad Software). Means between two groups were compared with two-tailed Student’s t test. Comparisons of means from multiple groups with each other or against one control group were analyzed with 1-way ANOVA followed by appropriate post-hoc tests.

CHAPTER 5:

DISCUSSION

5.1 Exosomes

We have shown that exosomes are important in regulating microglia responses to acute and chronic inflammation. Moreover, we identified exosome-mediated release of miR-155 as a mechanism of inflammatory resolution in activated microglia. Despite these striking findings, there is still much work to be done to fully understand the role of exosomes in microglia physiology given the heterogeneity of exosome content and the dynamicity of exosome release and uptake.

Some outstanding questions that arise from the work done to date are as follows. First, what additional mechanisms are involved in exosome regulation of microglia activation? This question can be answered using multiple approaches. For one, microglia can be isolated from ashen mice, which have a loss of function mutation in the *rab27a* gene, stimulated and then processed for RNA sequencing to identify differentially activated gene expression modules. These networks can then be investigated using more targeted molecular approaches to identify central regulators driving any observed phenotypic deviations. A caveat to this approach would be the utilization of *in vitro* microglia cultures. An alternative approach would be to perform the stimulations in live mice, through intraperitoneal or stereotaxic injections of activating agents. Since peripheral immune cells also express *rab27a*, stereotaxic injections will help circumvent any confounding effects brought about by loss of rab27a function in these cells. Alternatively, mice could be subjected to treatment with GW4869 over the course of one month and then treated with several inflammatory agents before microglia are isolated for downstream analyses. In all, these experiments are plagued by issues of lack of cell specificity. Development of floxed *rab27a* or *nSMase2* mouse lines will allow utilization of

Cre inducible systems to more specifically interrogate exosome function in different brain cells including microglia.

The second major question that arises is: what are other functions of exosomes in brain and microglia aging? Microglia from aged brains have been reported to show stronger anti-inflammatory and pro-neurogenic transcriptional signatures than to microglia from young brains [8]. Given our data showing augmented exosome production and its regulatory role in aged microglia inflammation, one could ask to what extent exosomes contribute to broad anti-inflammatory expression transcriptional signatures in aged microglia. Additionally, the presence of exosomes in the brain extracellular and the observed ability of exosomes to alter gene expression raises questions about their role in environmental regulation of microglia phenotype. Microglia regional diversity has been shown to change dramatically with age[55]. Augmented release of exosomes in aged microglia can potentially affect cellular phenotype either by acting as direct signaling molecules or regulating the cellular abundance of molecules driving specific phenotypes.

Finally, the third major question raised by is how exosomes are involved in microglia inflammation in the context of disease. Other studies have demonstrated exosome involvement in various brain disease processes including propagation of tau pathology in Alzheimer's disease (AD) [39] and microenvironmental reprogramming in glioma [33]. In AD particularly, exosomes have been implicated in the release of toxic amyloid and tau, with microglia involved in prion-like propagation of tau[39]. Given our study and the prominence of chronic inflammation in these diseases, it is likely that exosomes are also involved in regulating microglia activation in the disease brain. These disease states are likely to drive expanded functionality in exosomes due to differences in disease

etiology[90] and cellular responses[91]. Two potential areas in which expanded exosome functionality could manifest are as follows. First, stronger alteration of brain homeostasis and recruitment of pathological proteins might result in exosomes being more effective as direct mediators of intercellular inflammation compared to our observations in the non-diseased brain. Secondly, we show that exosome production is enhanced following experimentally induced lysosomal dysfunction. Changes in lysosome numbers and function have been identify in neurons and microglia in various models of AD[92,93]. It is unclear if endolysosomal dysfunction in AD drives any compensatory changes in exosome production machinery and how these might affect disease pathogenesis.

5.2 MicroRNA function in adult microglia

Our study demonstrated that microRNAs regulate a broad range of physiological functions in adult microglia, including survival, repopulation, inflammatory activation and morphology. In addition, depletion of dicer expression in adult microglia alters the hippocampal stem cell niche, with mutant hippocampi containing fewer neuronal progenitors and immature neurons compared to controls. These findings identify dicer-mediated miRNA production as a critical molecular mechanism involved in microglia and hippocampal homeostasis. Several questions arise based on our observations.

First, what miRNAs or miRNA targets are responsible for the observed phenotypic changes in dicer-depleted microglia? Our preliminary RNA sequencing experiment suggest a complex regulation of inflammation by dicer, with both pro- and anti-inflammatory pathways undergoing significant changes. To identify potential mediators of these inflammatory signature, we plan on performing miRNA sequencing on dicer-

depleted and control microglia. Comparison of gene targets of top differentially expressed miRNAs to differentially expressed gene transcripts identified in our initial profile will provide a comprehensive platform for assessing the relationship between miRNA changes and gene expression changes in dicer-depleted and control microglia. Through this, it will be possible to establish miRNA-mRNA combinations that can be probed using molecular knockdown approaches to determine their contributions to microglia survival, morphology and activation. This approach holds great potential for providing a more comprehensive view of microglia inflammatory regulation to include specific miRNAs that act as post transcriptional regulators.

Secondly, it is unclear how dicer-depletion in microglia is driving changes in the hippocampal stem cell niche. This question can be addressed by performing direct and indirect *in vitro* cocultures of wildtype hippocampal stem cells with dicer-depleted or control microglia. Indeed, microglia have been shown to regulate hippocampal stem cells through contact and production of secreted factors[94,95]. The proposed experimental approach can potentially identify new microglia secretory factors involved in regulation of stem cell number. It is also possible that the observed effect on stem cell number is associated with reduced microglia numbers. In that case, microglia depletion can be performed using other methods such as inhibition of colony stimulating factor 1 receptor signaling[78] or diphtheria toxin driving microglia apoptosis[96]. Comparison of all three models will help clarify if a critical number of microglia are needed for maintenance of the adult hippocampal stem cell niche.

BIBLIOGRAPHY

1 Ginhoux, F. *et al.* Fate mapping analysis reveals that adult microglia derive from primitive macrophages. *Science* **330**, 841-845, doi:10.1126/science.1194637 (2010).

2 Gomez Perdiguero, E. *et al.* Tissue-resident macrophages originate from yolk-sac-derived erythro-myeloid progenitors. *Nature* **518**, 547-551, doi:10.1038/nature13989 (2015).

3 Kierdorf, K. *et al.* Microglia emerge from erythromyeloid precursors via Pu.1- and Irf8-dependent pathways. *Nat Neurosci* **16**, 273-280, doi:10.1038/nn.3318 (2013).

4 Prinz, M. & Priller, J. Microglia and brain macrophages in the molecular age: from origin to neuropsychiatric disease. *Nat Rev Neurosci* **15**, 300-312, doi:10.1038/nrn3722 (2014).

5 Matcovitch-Natan, O. *et al.* Microglia development follows a stepwise program to regulate brain homeostasis. *Science* **353**, aad8670, doi:10.1126/science.aad8670 (2016).

6 Gosselin, D. *et al.* Environment drives selection and function of enhancers controlling tissue-specific macrophage identities. *Cell* **159**, 1327-1340, doi:10.1016/j.cell.2014.11.023 (2014).

7 Butovsky, O. *et al.* Identification of a unique TGF-beta-dependent molecular and functional signature in microglia. *Nat Neurosci* **17**, 131-143, doi:10.1038/nn.3599 (2014).

8 Hickman, S. E. *et al.* The microglial sensome revealed by direct RNA sequencing. *Nat Neurosci* **16**, 1896-1905, doi:10.1038/nn.3554 (2013).

9 Parkhurst, C. N. *et al.* Microglia promote learning-dependent synapse formation through brain-derived neurotrophic factor. *Cell* **155**, 1596-1609, doi:10.1016/j.cell.2013.11.030 (2013).

10 Jung, S. *et al.* Analysis of fractalkine receptor CX(3)CR1 function by targeted deletion and green fluorescent protein reporter gene insertion. *Mol Cell Biol* **20**, 4106-4114 (2000).

11 Nimmerjahn, A., Kirchhoff, F. & Helmchen, F. Resting microglial cells are highly dynamic surveillants of brain parenchyma in vivo. *Science* **308**, 1314-1318, doi:10.1126/science.1110647 (2005).

12 Davalos, D. *et al.* ATP mediates rapid microglial response to local brain injury in vivo. *Nat Neurosci* **8**, 752-758, doi:10.1038/nn1472 (2005).

13 Schafer, D. P. *et al.* Microglia sculpt postnatal neural circuits in an activity and complement-dependent manner. *Neuron* **74**, 691-705, doi:10.1016/j.neuron.2012.03.026 (2012).

14 Li, Y., Du, X. F., Liu, C. S., Wen, Z. L. & Du, J. L. Reciprocal regulation between resting microglial dynamics and neuronal activity in vivo. *Dev Cell* **23**, 1189-1202, doi:10.1016/j.devcel.2012.10.027 (2012).

15 Mosher, K. I. & Wyss-Coray, T. Microglial dysfunction in brain aging and Alzheimer's disease. *Biochem Pharmacol* **88**, 594-604, doi:10.1016/j.bcp.2014.01.008 (2014).

16 Udeochu, J. C., Shea, J. M. & Villeda, S. A. Microglia communication: Parallels between aging and Alzheimer's disease. *Clin Exp Neuroimmunol* **7**, 114-125, doi:10.1111/cen3.12307 (2016).

17 Ye, S. M. & Johnson, R. W. Increased interleukin-6 expression by microglia from brain of aged mice. *J Neuroimmunol* **93**, 139-148 (1999).

18 Sierra, A., Gottfried-Blackmore, A. C., McEwen, B. S. & Bulloch, K. Microglia derived from aging mice exhibit an altered inflammatory profile. *Glia* **55**, 412-424, doi:10.1002/glia.20468 (2007).

19 Cho, S. H. *et al.* SIRT1 deficiency in microglia contributes to cognitive decline in aging and neurodegeneration via epigenetic regulation of IL-1beta. *J Neurosci* **35**, 807-818, doi:10.1523/jneurosci.2939-14.2015 (2015).

20 Reichwald, J., Danner, S., Wiederhold, K. H. & Staufenbiel, M. Expression of complement system components during aging and amyloid deposition in APP transgenic mice. *J Neuroinflammation* **6**, 35, doi:10.1186/1742-2094-6-35 (2009).

21 Fu, H. *et al.* Complement component C3 and complement receptor type 3 contribute to the phagocytosis and clearance of fibrillar Abeta by microglia. *Glia* **60**, 993-1003, doi:10.1002/glia.22331 (2012).

22 Cribbs, D. H. *et al.* Extensive innate immune gene activation accompanies brain aging, increasing vulnerability to cognitive decline and neurodegeneration: a microarray study. *J Neuroinflammation* **9**, 179, doi:10.1186/1742-2094-9-179 (2012).

23 Benoit, M. E. *et al.* C1q-induced LRP1B and GPR6 proteins expressed early in Alzheimer disease mouse models, are essential for the C1q-mediated protection against amyloid-beta neurotoxicity. *J Biol Chem* **288**, 654-665, doi:10.1074/jbc.M112.400168 (2013).

24 Lui, H. *et al.* Progranulin Deficiency Promotes Circuit-Specific Synaptic Pruning by Microglia via Complement Activation. *Cell* **165**, 921-935, doi:10.1016/j.cell.2016.04.001 (2016).

25 Hong, S. *et al.* Complement and microglia mediate early synapse loss in Alzheimer mouse models. *Science* **352**, 712-716, doi:10.1126/science.aad8373 (2016).

26 Damani, M. R. *et al.* Age-related alterations in the dynamic behavior of microglia. *Aging Cell* **10**, 263-276, doi:10.1111/j.1474-9726.2010.00660.x (2011).

27 Hefendehl, J. K. *et al.* Homeostatic and injury-induced microglia behavior in the aging brain. *Aging Cell* **13**, 60-69, doi:10.1111/acel.12149 (2014).

28 Thery, C. Exosomes: secreted vesicles and intercellular communications. *F1000 Biol Rep* **3**, 15, doi:10.3410/B3-15 (2011).

29 Fruhbeis, C. *et al.* Neurotransmitter-triggered transfer of exosomes mediates oligodendrocyte-neuron communication. *PLoS Biol* **11**, e1001604, doi:10.1371/journal.pbio.1001604 (2013).

30 Fitzner, D. *et al.* Selective transfer of exosomes from oligodendrocytes to microglia by macropinocytosis. *J Cell Sci* **124**, 447-458, doi:10.1242/jcs.074088 (2011).

31 Zappulli, V., Friis, K. P., Fitzpatrick, Z., Maguire, C. A. & Breakefield, X. O. Extracellular vesicles and intercellular communication within the nervous system. *J Clin Invest* **126**, 1198-1207, doi:10.1172/JCI81134 (2016).

32 Vella, L. J., Sharples, R. A., Nisbet, R. M., Cappai, R. & Hill, A. F. The role of exosomes in the processing of proteins associated with neurodegenerative diseases. *Eur Biophys J* **37**, 323-332, doi:10.1007/s00249-007-0246-z (2008).

33 Skog, J. *et al.* Glioblastoma microvesicles transport RNA and proteins that promote tumour growth and provide diagnostic biomarkers. *Nat Cell Biol* **10**, 1470-1476, doi:10.1038/ncb1800 (2008).

34 Rajendran, L. *et al.* Emerging roles of extracellular vesicles in the nervous system. *J Neurosci* **34**, 15482-15489, doi:10.1523/JNEUROSCI.3258-14.2014 (2014).

35 Zhang, L. *et al.* Microenvironment-induced PTEN loss by exosomal microRNA primes brain metastasis outgrowth. *Nature* **527**, 100-104, doi:10.1038/nature15376 (2015).

36 Coleman, B. M. & Hill, A. F. Extracellular vesicles--Their role in the packaging and spread of misfolded proteins associated with neurodegenerative diseases. *Semin Cell Dev Biol* **40**, 89-96, doi:10.1016/j.semcdb.2015.02.007 (2015).

37 Perez-Gonzalez, R., Gauthier, S. A., Kumar, A. & Levy, E. The exosome secretory pathway transports amyloid precursor protein carboxyl-terminal fragments from the cell into the brain extracellular space. *J Biol Chem* **287**, 43108-43115, doi:10.1074/jbc.M112.404467 (2012).

38 Dinkins, M. B., Dasgupta, S., Wang, G., Zhu, G. & Bieberich, E. Exosome reduction in vivo is associated with lower amyloid plaque load in the 5XFAD mouse model of Alzheimer's disease. *Neurobiol Aging* **35**, 1792-1800, doi:10.1016/j.neurobiolaging.2014.02.012 (2014).

39 Asai, H. *et al.* Depletion of microglia and inhibition of exosome synthesis halt tau propagation. *Nat Neurosci* **18**, 1584-1593, doi:10.1038/nn.4132 (2015).

40 Zhang, Y. *et al.* Hypothalamic stem cells control ageing speed partly through exosomal miRNAs. *Nature* **548**, 52-57, doi:10.1038/nature23282 (2017).

41 Thery, C., Ostrowski, M. & Segura, E. Membrane vesicles as conveyors of immune responses. *Nat Rev Immunol* **9**, 581-593, doi:10.1038/nri2567 (2009).

42 Raposo, G. & Stoorvogel, W. Extracellular vesicles: exosomes, microvesicles, and friends. *J Cell Biol* **200**, 373-383, doi:10.1083/jcb.201211138 (2013).

43 Potolicchio, I. *et al.* Proteomic analysis of microglia-derived exosomes: metabolic role of the aminopeptidase CD13 in neuropeptide catabolism. *J Immunol* **175**, 2237-2243 (2005).

44 Bianco, F. *et al.* Acid sphingomyelinase activity triggers microparticle release from glial cells. *EMBO J* **28**, 1043-1054, doi:10.1038/emboj.2009.45 (2009).

45 Guduric-Fuchs, J. *et al.* Selective extracellular vesicle-mediated export of an overlapping set of microRNAs from multiple cell types. *BMC Genomics* **13**, 357, doi:10.1186/1471-2164-13-357 (2012).

46 Barca-Mayo, O. & Lu, Q. R. Fine-Tuning Oligodendrocyte Development by microRNAs. *Front Neurosci* **6**, 13, doi:10.3389/fnins.2012.00013 (2012).

47 Drinnenberg, I. A. *et al.* RNAi in budding yeast. *Science* **326**, 544-550, doi:10.1126/science.1176945 (2009).

48 Bernstein, E. *et al.* Dicer is essential for mouse development. *Nat Genet* **35**, 215-217, doi:10.1038/ng1253 (2003).

49 Valadi, H. *et al.* Exosome-mediated transfer of mRNAs and microRNAs is a novel mechanism of genetic exchange between cells. *Nat Cell Biol* **9**, 654-659, doi:10.1038/ncb1596 (2007).

50 Okoye, I. S. *et al.* MicroRNA-containing T-regulatory-cell-derived exosomes suppress pathogenic T helper 1 cells. *Immunity* **41**, 89-103, doi:10.1016/j.immuni.2014.05.019 (2014).

51 Gibbings, D. J., Ciaudo, C., Erhardt, M. & Voinnet, O. Multivesicular bodies associate with components of miRNA effector complexes and modulate miRNA activity. *Nat Cell Biol* **11**, 1143-1149, doi:10.1038/ncb1929 (2009).

52 Kettenmann, H., Hanisch, U. K., Noda, M. & Verkhratsky, A. Physiology of microglia. *Physiol Rev* **91**, 461-553, doi:10.1152/physrev.00011.2010 (2011).

53 Davies, L. C. & Taylor, P. R. Tissue-resident macrophages: then and now. *Immunology* **144**, 541-548, doi:10.1111/imm.12451 (2015).

54 Epelman, S., Lavine, K. J. & Randolph, G. J. Origin and functions of tissue macrophages. *Immunity* **41**, 21-35, doi:10.1016/j.immuni.2014.06.013 (2014).

55 Grabert, K. *et al.* Microglial brain region-dependent diversity and selective regional sensitivities to aging. *Nat Neurosci* **19**, 504-516, doi:10.1038/nn.4222 (2016).

56 Prinz, M., Priller, J., Sisodia, S. S. & Ransohoff, R. M. Heterogeneity of CNS myeloid cells and their roles in neurodegeneration. *Nat Neurosci* **14**, 1227-1235, doi:10.1038/nn.2923 (2011).

57 Thery, C. *et al.* Indirect activation of naive CD4+ T cells by dendritic cell-derived exosomes. *Nat Immunol* **3**, 1156-1162, doi:10.1038/ni854 (2002).

58 Montecalvo, A. *et al.* Mechanism of transfer of functional microRNAs between mouse dendritic cells via exosomes. *Blood* **119**, 756-766, doi:10.1182/blood-2011-02-338004 (2012).

59 Thery, C., Amigorena, S., Raposo, G. & Clayton, A. Isolation and characterization of exosomes from cell culture supernatants and biological fluids. *Curr Protoc Cell Biol* **Chapter 3**, Unit 3 22, doi:10.1002/0471143030.cb0322s30 (2006).

60 Simpson, R. J., Kalra, H. & Mathivanan, S. ExoCarta as a resource for exosomal research. *J Extracell Vesicles* **1**, doi:10.3402/jev.v1i0.18374 (2012).

61 Blank, T. & Prinz, M. Type I interferon pathway in CNS homeostasis and neurological disorders. *Glia* **65**, 1397-1406, doi:10.1002/glia.23154 (2017).

62 Baruch, K. *et al.* Aging. Aging-induced type I interferon response at the choroid plexus negatively affects brain function. *Science* **346**, 89-93, doi:10.1126/science.1252945 (2014).

63 Filiano, A. J. *et al.* Unexpected role of interferon-gamma in regulating neuronal connectivity and social behaviour. *Nature* **535**, 425-429, doi:10.1038/nature18626 (2016).

64 Bialas, A. R. *et al.* Microglia-dependent synapse loss in type I interferon-mediated lupus. *Nature* **546**, 539-543, doi:10.1038/nature22821 (2017).

65 Jovicic, A. *et al.* Comprehensive expression analyses of neural cell-type-specific miRNAs identify new determinants of the specification and maintenance of neuronal phenotypes. *J Neurosci* **33**, 5127-5137, doi:10.1523/JNEUROSCI.0600-12.2013 (2013).

66 Varol, D. *et al.* Dicer Deficiency Differentially Impacts Microglia of the Developing and Adult Brain. *Immunity* **46**, 1030-1044 e1038, doi:10.1016/j.immuni.2017.05.003 (2017).

67 Song, M. M. & Shuai, K. The suppressor of cytokine signaling (SOCS) 1 and SOCS3 but not SOCS2 proteins inhibit interferon-mediated antiviral and antiproliferative activities. *J Biol Chem* **273**, 35056-35062 (1998).

68 Ponomarev, E. D., Veremeyko, T. & Weiner, H. L. MicroRNAs are universal regulators of differentiation, activation, and polarization of microglia and macrophages in normal and diseased CNS. *Glia* **61**, 91-103, doi:10.1002/glia.22363 (2013).

69 Wang, P. *et al.* Inducible microRNA-155 feedback promotes type I IFN signaling in antiviral innate immunity by targeting suppressor of cytokine signaling 1. *J Immunol* **185**, 6226-6233, doi:10.4049/jimmunol.1000491 (2010).

70 Parchem, R. J. *et al.* miR-302 Is Required for Timing of Neural Differentiation, Neural Tube Closure, and Embryonic Viability. *Cell Rep* **12**, 760-773, doi:10.1016/j.celrep.2015.06.074 (2015).

71 Montoya, M. M. *et al.* A Distinct Inhibitory Function for miR-18a in Th17 Cell Differentiation. *J Immunol* **199**, 559-569, doi:10.4049/jimmunol.1700170 (2017).

72 Dulcis, D. *et al.* Neurotransmitter Switching Regulated by miRNAs Controls Changes in Social Preference. *Neuron*, doi:10.1016/j.neuron.2017.08.023 (2017).

73 Ponomarev, E. D., Veremeyko, T., Barteneva, N., Krichevsky, A. M. & Weiner, H. L. MicroRNA-124 promotes microglia quiescence and suppresses EAE by deactivating macrophages via the C/EBP-alpha-PU.1 pathway. *Nat Med* **17**, 64-70, doi:10.1038/nm.2266 (2011).

74 Butovsky, O. *et al.* Targeting miR-155 restores abnormal microglia and attenuates disease in SOD1 mice. *Ann Neurol* **77**, 75-99, doi:10.1002/ana.24304 (2015).

75 Harfe, B. D., McManus, M. T., Mansfield, J. H., Hornstein, E. & Tabin, C. J. The RNaseIII enzyme Dicer is required for morphogenesis but not patterning of the vertebrate limb. *Proc Natl Acad Sci U S A* **102**, 10898-10903, doi:10.1073/pnas.0504834102 (2005).

76 Goldmann, T. *et al.* A new type of microglia gene targeting shows TAK1 to be pivotal in CNS autoimmune inflammation. *Nat Neurosci* **16**, 1618-1626, doi:10.1038/nn.3531 (2013).

77 Mattis, A. N. *et al.* A screen in mice uncovers repression of lipoprotein lipase by microRNA-29a as a mechanism for lipid distribution away from the liver. *Hepatology* **61**, 141-152, doi:10.1002/hep.27379 (2015).

78 Elmore, M. R. *et al.* Colony-stimulating factor 1 receptor signaling is necessary for microglia viability, unmasking a microglia progenitor cell in the adult brain. *Neuron* **82**, 380-397, doi:10.1016/j.neuron.2014.02.040 (2014).

79 Buttgereit, A. *et al.* Sall1 is a transcriptional regulator defining microglia identity and function. *Nat Immunol* **17**, 1397-1406, doi:10.1038/ni.3585 (2016).

80 Ransohoff, R. M. A polarizing question: do M1 and M2 microglia exist? *Nat Neurosci* **19**, 987-991, doi:10.1038/nn.4338 (2016).

81 Carpentier, P. A. & Palmer, T. D. Immune influence on adult neural stem cell regulation and function. *Neuron* **64**, 79-92, doi:10.1016/j.neuron.2009.08.038 (2009).

82 Bonaguidi, M. A., Song, J., Ming, G. L. & Song, H. A unifying hypothesis on mammalian neural stem cell properties in the adult hippocampus. *Curr Opin Neurobiol* **22**, 754-761, doi:10.1016/j.conb.2012.03.013 (2012).

83 Goncalves, J. T., Schafer, S. T. & Gage, F. H. Adult Neurogenesis in the Hippocampus: From Stem Cells to Behavior. *Cell* **167**, 897-914, doi:10.1016/j.cell.2016.10.021 (2016).

84 Raber, J. *et al.* Irradiation enhances hippocampus-dependent cognition in mice deficient in extracellular superoxide dismutase. *Hippocampus* **21**, 72-80, doi:10.1002/hipo.20724 (2011).

85 Alamed, J., Wilcock, D. M., Diamond, D. M., Gordon, M. N. & Morgan, D. Two-day radial-arm water maze learning and memory task; robust resolution of amyloid-related memory deficits in transgenic mice. *Nat Protoc* **1**, 1671-1679, doi:10.1038/nprot.2006.275 (2006).

86 Blasi, E., Barluzzi, R., Bocchini, V., Mazzolla, R. & Bistoni, F. Immortalization of murine microglial cells by a v-raf/v-myc carrying retrovirus. *J Neuroimmunol* **27**, 229-237 (1990).

87 Trombetta, J. J. *et al.* Preparation of Single-Cell RNA-Seq Libraries for Next Generation Sequencing. *Curr Protoc Mol Biol* **107**, 4 22 21-17, doi:10.1002/0471142727.mb0422s107 (2014).

88 Villeda, S. A. *et al.* The ageing systemic milieu negatively regulates neurogenesis and cognitive function. *Nature* **477**, 90-94, doi:10.1038/nature10357 (2011).

89 Lucin, K. M. *et al.* Microglial beclin 1 regulates retromer trafficking and phagocytosis and is impaired in Alzheimer's disease. *Neuron* **79**, 873-886, doi:10.1016/j.neuron.2013.06.046 (2013).

90 Orre, M. *et al.* Isolation of glia from Alzheimer's mice reveals inflammation and dysfunction. *Neurobiol Aging* **35**, 2746-2760, doi:10.1016/j.neurobiolaging.2014.06.004 (2014).

91 Keren-Shaul, H. *et al.* A Unique Microglia Type Associated with Restricting Development of Alzheimer's Disease. *Cell* **169**, 1276-1290 e1217, doi:10.1016/j.cell.2017.05.018 (2017).

92 Orr, M. E. & Oddo, S. Autophagic/lysosomal dysfunction in Alzheimer's disease. *Alzheimers Res Ther* **5**, 53, doi:10.1186/alzrt217 (2013).

93 Nixon, R. A. Amyloid precursor protein and endosomal-lysosomal dysfunction in Alzheimer's disease: inseparable partners in a multifactorial disease. *FASEB J* **31**, 2729-2743, doi:10.1096/fj.201700359 (2017).

94 Sierra, A. *et al.* Microglia shape adult hippocampal neurogenesis through apoptosis-coupled phagocytosis. *Cell Stem Cell* **7**, 483-495, doi:10.1016/j.stem.2010.08.014 (2010).

95 Vukovic, J., Colditz, M. J., Blackmore, D. G., Ruitenberg, M. J. & Bartlett, P. F. Microglia modulate hippocampal neural precursor activity in response to exercise and aging. *J Neurosci* **32**, 6435-6443, doi:10.1523/JNEUROSCI.5925-11.2012 (2012).

96 Bruttger, J. *et al.* Genetic Cell Ablation Reveals Clusters of Local Self-Renewing Microglia in the Mammalian Central Nervous System. *Immunity* **43**, 92-106, doi:10.1016/j.immuni.2015.06.012 (2015).

Publishing Agreement

It is the policy of the University to encourage the distribution of all theses, dissertations, and manuscripts. Copies of all UCSF theses, dissertations, and manuscripts will be routed to the library via the Graduate Division. The library will make all theses, dissertations, and manuscripts accessible to the public and will preserve these to the best of their abilities, in perpetuity.

Please sign the following statement:

I hereby grant permission to the Graduate Division of the University of California, San Francisco to release copies of my thesis, dissertation, or manuscript to the Campus Library to provide access and preservation, in whole or in part, in perpetuity.

Author Signature

09/27/17

Date